SEDIMENTOLOGY the journal of the International Association of Sedimentologists IAS

Sedimentology (2025) doi: 10.1111/sed.70035

Neoichnology and sediment distribution in tidal flats of the mud-dominated mesotidal Mira River estuary (Portugal)

ALINA SHCHEPETKINA* , TERESA DRAGO†'‡, JACQUELINE SANTOS†'‡'§, ANA ALBERTO‡'¶, FRANCISCO FATELA‡'¶ and MARIA DA CONCEIÇÃO FREITAS‡'¶

**Department of Earth Sciences, The University of Western Ontario, London, ON N6A 5B7, Canada (E-mail: ashchep@uwo.ca)*

†Instituto Português do Mar e da Atmosfera, I.P. (IPMA), Tavira 8800-737, Portugal

‡Faculdade de Ciências, Instituto Dom Luiz (IDL), Universidade de Lisboa, Lisbon 1740-016, Portugal

§Center de Investigação Marinha e Ambiental (CIMA), Universidade do Algarve, Campus de Gambelas, Faro 8005-139, Portugal

¶Departamento de Geologia, Faculdade de Ciências, Universidade de Lisboa, Lisbon 1740-016, Portugal

Associate Editor – Marc Aurell

ABSTRACT

Invertebrate burrow morphologies and distributions are presented for the tidal flats of the middle and lower reaches of the tide-influenced (mesotidal), mud-dominated Mira River estuary (SW Portugal) as an analogue for interpreting the ichnology of palaeoestuarine successions. Burrow distributions are revealed using field observations of biogenic and physical sedimentary structures, trace makers, collected grab samples, push cores and lab measurements of grain size, organic matter and calcium carbonate content and linked to physico-chemical stresses. Estuarine tidal-flat surface open burrow distribution and bioturbation intensity are analysed in plan view using free scientific image analysis software (ImageJ) to obtain burrow density, total burrow area and minimum and maximum burrow diameters. The total tidal flat area occupied by organisms ranges from 0.8% to 4.1% in the middle estuary and is 1.4% in the lower estuary. These equate to a bioturbation index of one to two (BI 1–2). However, computed tomography (CT) of push cores (cross-sectional view) taken on the same tidal flats shows sparse to complete bioturbation intensity (BI 1–6), revealing that tidal flat sediments tend to be more biogenically reworked cumulatively over time with overprinting of subsequent tiers and/or recolonized. CT scanning also allows the identification of more burrow types, demonstrates infaunal tiering and provides insights into trace-fossil preservation potential. This research shows that the trace communities are heterogeneous and change spatially and temporally along the Mira River estuary, reflecting a physico-chemical gradient and seasonality. This trend signals changes in sediment composition, substrate type and consistency (sediment compaction and subaerial exposure), salinity, oxygenation, temperature, pH and interplay of tidal versus hydraulic energy.

Keywords coastal sedimentation, computed tomography, digital image analysis, infauna, physico-chemical stress.

INTRODUCTION

The present-day knowledge of traces in brackish-water environments predominantly comes from scrutinizing the behaviour of trace makers and their resultant biogenic structures in modern and Holocene depositional systems (e.g. Pemberton *et al.*, 1982; Beynon *et al.*, 1988; Gingras *et al.*, 1999; Buatois *et al.*, 2005; Wetzel *et al.*, 2017; Wetzel & Unverricht, 2020; Gingras *et al.*, 2025). Studying present-day analogues offers a robust foundation for understanding the relationships between known environmental factors (e.g. salinity, hydraulic energy, turbidity, temperature, pH, oxygen saturation, substrate texture and composition) and trace characteristics (e.g. Elders, 1975; MacEachern *et al.*, 2012; La Croix *et al.*, 2022). This knowledge can then be applied to the rock and sediment record (e.g. Gingras *et al.*, 1999; Buatois *et al.*, 2005; Dashtgard *et al.*, 2008; Dashtgard, 2011a, 2011b; Gingras *et al.*, 2012). As such, neoichnological and sedimentological characterization of modern estuarine environments can also reveal trends that reflect changes in sediment grain size, subaerial exposure and sedimentation rate, among others (Dashtgard, 2011a; Gingras *et al.*, 2025). Neoichnological studies of estuaries, deltas and open tidal flats have been conducted since the 1920s in Northern Europe and later, since the 1950s, in North America. Some of the first studies come from the Wadden Sea, Germany (e.g. Richter, 1920; Schäfer, 1972) and the eastern coast of the USA (Frey & Mayou, 1971; Howard *et al.*, 1975; Howard & Frey, 1975; Frey *et al.*, 1984). Later studies concentrated on the Fraser River delta, BC, Canada (e.g. Swinbanks, 1981; Swinbanks & Murray, 1981; Swinbanks & Luternauer, 1987; Luternauer *et al.*, 1995; Dashtgard, 2011a, 2011b; Ayranci *et al.*, 2014), Willapa Bay, WA, USA (e.g. Gingras *et al.*, 1999, 2002a; Schoengut, 2011; Gingras *et al.*, 2014), Tillamook Bay, OR, USA (Bistran, 2014), Bay of Fundy area, NS and NB, Canada (Pearson, 2006; Pearson & Gingras, 2006; Hauck, 2008; Hauck *et al.*, 2009; Dashtgard *et al.*, 2014; Shchepetkina *et al.*, 2016c), and Ogeechee River estuary, GA, USA (Gunn *et al.*, 2008; Shchepetkina *et al.*, 2016a). To the best of our knowledge, no neoichnological studies have been conducted in Portugal, except for a few recent studies on the CT scanning of the Mira River estuary tidal flats (Shchepetkina *et al.*, 2023) and preserved crab traces on tidal flats (Shchepetkina, 2025).

Trace fossil assemblages formed in estuarine settings are characterized by the brackish-water ichnological model (Pemberton *et al.*, 1982; Wightman *et al.*, 1987; Beynon *et al.*, 1988; Maceachern & Pemberton, 1994; Buatois *et al.*, 2005; MacEachern & Gingras, 2007), and have been described as 'mixed *Cruziana–Skolithos* ichnofacies' (e.g. Greb & Chesnut, 1994; Hovikoski *et al.*, 2007) and as 'depauperate *Cruziana* Ichnofacies' (e.g. Solárzano *et al.*, 2017; Zhang *et al.*, 2017). However, recently, Gingras *et al.* (2025) have erected a new ichnofacies for trace fossil assemblages of paralic to shallow-marine, persistently brackish-water environments and termed it the *Teichichnus* Ichnofacies. This ichnofacies mainly reflects the response to reduced salinity and tidal processes that dictate the sporadic (temporally and spatially) food resource distribution. The *Teichichnus* Ichnofacies is defined by trace diminution, reduced trace diversity (typically 1 to 4 ichnogenera), especially with increasing physico-chemical stress, permanent structures for surface deposit feeding, intrastratal deposit feeding, lesser for filter feeding, variable bioturbation intensity (BI 0 to 6) and opportunistic infaunal behaviour with top-down colonization due to rapid deposition of event beds. Both Buatois *et al.* (2005) and Gingras *et al.* (2025), based on neoichnological studies, also point out that, modern brackish-water deposits are typified by: (1) high diversity of burrowing animals in the lower and middle reaches of the estuaries, and lower diversity of burrowing infauna in the upper estuary; (2) high bioturbation intensity within sediments, unless the biota is overwhelmed by stresses like high water turbidity and/or lowered oxygenation; (3) the predominance of traces created by polychaetes, molluscs and crustaceans; (4) a wide variety of substrate types present (i.e. softground, stiffground, firmground, hardground and woodground); and (5) the prevalence of opportunistic behaviours of infauna necessary to overcome stressful environmental conditions.

As neoichnological trends are considered an excellent proxy for the interpretation of sedimentary environments in the rock and sedimentary record (Dashtgard, 2011a), studies linking physico-chemical stresses with burrow architecture (i.e. morphology and internal structure of burrows) and the ichnological character of sediments (i.e. bioturbation intensity, trace diversity, tiering and

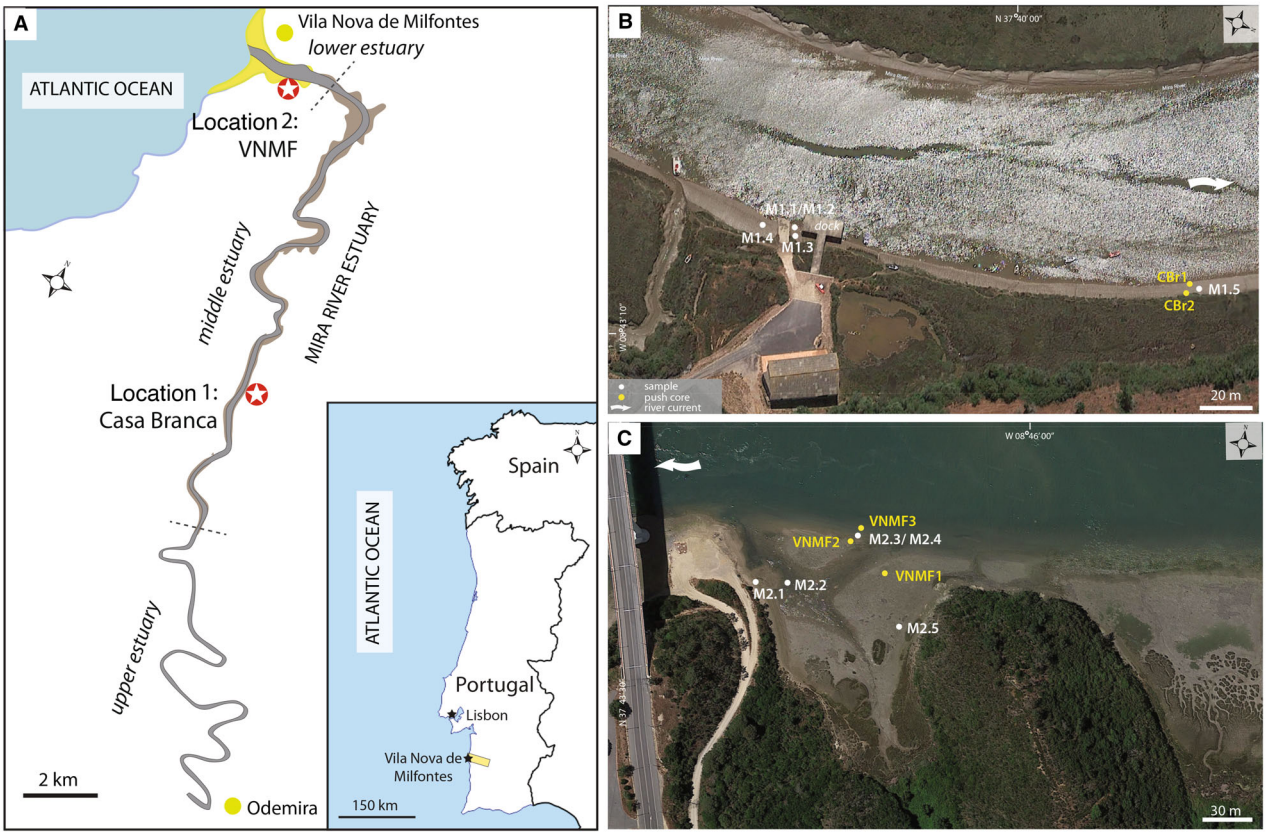

Fig. 1. (A) Location of study sites in the Mira River estuary. Inset: Regional map of the Iberian Peninsula showing the location of the study area in southwestern Portugal. (B) Satellite image of the Casa Branca (CBr) middle estuary study site showing the location of grab samples (in white), two push cores (in yellow) and the direction of the fluvial current (white arrow). Site 1: samples M1.1–M1.3; Site 2: sample M1.4; Site 3: sample M1.5, push cores CBR1T.F-CBR2T.F. (C) Satellite image of the Vila Nova de Milfontes (VNMF) lower estuary study site showing the location of grab samples (in white), three push cores (in yellow) and the direction of the fluvial current (white arrow). Site 1: samples M2.1–M2.2; Site 2: push core VNMF1; Site 3: samples M2.3–M2.4, push cores VNMF2–3; Site 4: sample M2.5. For more details, see Fig. 2.

ichnofacies) are still critically needed. Herein, sedimentological, neoichnological and physico-chemical trends for the tidal flats of the lower to middle mesotidal Mira River estuary in SW Portugal are established. Such an assessment reveals the importance of various physico-chemical (e.g. salinity, turbidity and pH) and biotic stresses (e.g. predation pressure, competition for space and resources, seasonal or lifecycle behaviours) imposed on the resulting neoichnological assemblage. Distributions of individual taxa and bioturbation intensity derived from the estuarine tidal-flat surfaces (horizontal section) are calculated and compared to those of push cores (vertical section) using computed tomography (CT).

STUDY AREA

The Mira River estuary is a narrow, almost pristine coastal plain estuary in the Sudoeste Alentejano e Costa Vicentina Natural Park, SW Portugal (Fig. 1A; Blanton *et al.*, 2000; Castro & Freitas, 2006; Adão *et al.*, 2009; Duarte *et al.*, 2020) surrounded by 285 ha of salt marshes (Costa *et al.*, 2001). The Mira River originates in the Serra do Caldeirão and flows northwards for 145 km, reaching the Atlantic Ocean close to Vila Nova de Mil Fontes at 37°43′08″N, 08°47′17″W (e.g. Blanton *et al.*, 2000). Its watershed constitutes approximately 1600 km^2, with sediment supplied from the source rocks representing greywackes, pelites, slates, schists and

conglomerates (e.g. Fatela *et al.*, 2016; Moreno *et al.*, 2017). The estuary is up to 400 m wide near the mouth and 70 to 75 m in its middle part, while depth varies from 20 m to 3–5 m sailing upstream along these zones (Ré, 1996; Picado *et al.*, 2020).

The Mira River estuary is mesotidal whose semi-diurnal tides record a mean tidal range of 2.4 m, neap tides of 1 to 2 m and a maximum tidal range of 3.5 m (e.g. Blanton & Andrade, 2001; Paula *et al.*, 2006; Amaral *et al.*, 2007; Moreno *et al.*, 2017; Duarte *et al.*, 2020; Picado *et al.*, 2020). The estuary is tide-influenced and is characterized by flood tidal dominance, allowing the landward transport of well-oxygenated water coupled with high residence times (Picado *et al.*, 2020). The highest residence times have been noted for the middle estuary, reaching 12 days in winter and 50 days in summer (Picado *et al.*, 2020). The salt wedge propagates up to 32 km upstream in summer (e.g. Bettencourt *et al.*, 2004; Moreno *et al.*, 2017, 2019), and the dynamic tide extends almost 40 km inland (Costa *et al.*, 2001). The area is characterized by a Koppen Csb climate type, with a mean annual precipitation of 645 mm and hot summers with mean annual temperatures of 25 to 28°C (e.g. Fatela *et al.*, 2016). Freshwater inflow is seasonal and low (2.9 to 10 m^3/s), and nearly 0 m^3/s in dry years (Costa *et al.*, 2001; Ferreira *et al.*, 2003). River discharge is mainly controlled by an irrigation dam located upstream (Costa *et al.*, 2001). High river discharge, averaging 18 m^3/s and reaching 500 m^3/s during rainy seasons, occurs from January to February and April, whereas low fluvial discharge is typical for July to August and October to November when it drops to 1 m^3/s (Blanton *et al.*, 2000; Blanton & Andrade, 2001; Fatela *et al.*, 2016; Duarte *et al.*, 2020). The estuary is vertically homogeneous during spring tides and slightly stratified during neap tides (Paula, 1998; Blanton & Andrade, 2001). Salinity in the Mira River estuary is highly variable, depending on the season and fluvial discharge, and the lower estuary is normally characterized by mesohaline to euhaline water salinities (15 to 36‰; Paula, 1998; Blanton & Andrade, 2001; Costa *et al.*, 2001; Fatela *et al.*, 2016), whereas in the upper reaches, salinities range from 0.5 to 5‰ (Paula, 1998; Adão *et al.*, 2009). Despite being relatively undisturbed by anthropogenic activities, the estuary experiences pollution due to agricultural, breeding and aquacultural activities, as well as urban wastewater discharge and seasonal tourism (Costa *et al.*, 2001; Castro & Freitas, 2006).

Two locations (with three to four sites each) were selected for this study. These are situated along the intertidal flats of the middle and lower Mira River estuary, as defined by water salinity gradient and residence times (Picado *et al.*, 2020), and are bordered by salt marshes. The middle estuary location is situated ~11 km upstream from the estuary entrance on the muddy tidal flats of Casa Branca (CBr, Location 1, Fig. 1A, B), while the lower estuary location lies 2 km upstream from the estuary entrance near Vila Nova de Milfontes (VNMF, Location 2, Fig. 1A to C).

METHODS

Fieldwork was carried out from 30 to 31 June 2021, at neap low tide (1.29 m). Data collection in the field included: (1) surficial observations of physical and biogenic sedimentary structures; (2) observations of burrow morphology and infaunal organisms in shallow trenches; (3) *in situ* measurements of water salinity, dissolved oxygen, temperature and pH at low and high slack-water periods; (4) collection of surficial grab samples and ~1 m long push cores; (5) field photography; and (6) thickness measurements of the fluid mud layer. Field photography was accomplished using a Canon PowerShot G1 X with the following settings: 180 × 180 resolution, RGB colour space, ISO 200, exposure time 1/1250, focal length 15.1 mm and a 15.1 to 60.4 mm lens. Water salinity (‰), temperature (°C), pH and dissolved oxygen (%) were measured using the WTW Cond 197i and WTW Oxi 197i probes. The pH probe revealed a misfunction in the field. Therefore, the average pH measured at the same sites during the historically comparably low-flow seasons in April 2006, May 2007 and November 2019 was calculated. One to three surficial (0 to 1 cm depth) grab sediment samples, with a total of 10, were taken at each station along the depositional profile. Each grab sample represented approximately 100 to 200 mL in volume, roughly equivalent to a handful of sediment. Push coring was conducted using 3″ (7.5 cm), 50 cm long PVC pipes: Two push cores were collected from the tidal flat of the middle estuary, and three push cores were obtained from the lower estuary tidal flat. While the core depth varied depending on substrate resistance, the cores reached the depths of 37 to

50 cm. After collection, push cores were capped and kept in a cool chamber (IPMA Tavira) at 4°C to preserve moisture and avoid diagenetic alterations and sediment desiccation.

Laboratory methods included: (1) grain size, organic matter and total calcium carbonate content analyses on grab samples and push cores (with a 3-cm step); (2) computed tomography (CT scanning) of whole-round cores; and (3) daylight photography and core logging of all split cores.

The coarse-grained fraction of the grab samples (0.063 to 2 mm) was analysed using a set of standard laboratory test sieves (Retsch D-42759, Germany). Eight classes of sediment calibres were measured from silt and clay (<0.063 mm) to pebble sizes (>4 mm). The fine-grained fraction (<0.063 mm) of the grab samples was then sub-sampled and analysed on a laser diffraction particle size analyser Malvern Hydro 2000 MU (Faculty of Sciences, University of Lisbon), where the samples were treated with 10% potassium hydroxide to dissolve organic material and deflocculated using 30% sodium hexametaphosphate. The procedure for fine-grained measurements using Malvern Hydro 2000 was as follows: (1) 0.08 g of each sample was diluted with ~20 mL of deionized water and 1 to 2 mL of sodium hexametaphosphate; (2) diluted samples were vigorously mixed and left to stand for 20 to 24 h; (3) samples were passed through an ultrasonic bath (Transsonic T820/H) for 1 to 3 min; and finally, (4) five measurements of each sample were taken in a Malvern water chamber, and the average of these five passes was calculated. Granulometric analysis of the push cores was conducted using a laser diffraction particle size analyser (Malvern Mastersizer 3000) coupled with an automated wet dispersion unit (Hydro LV; IPMA station, Tavira, Algarve). Prior to analysis with the Malvern Mastersizer 3000, the samples were also treated with 10% potassium hydroxide to dissolve organic material and deflocculated in 10 mL of deionized water with 3 to 4 drops of 30% sodium hexametaphosphate before repetitively measuring each sample in a water chamber. The average of five passes was used for grain-size analysis. Based on the clay, silt, sand and gravel percentages, the sediments were classified following Folk (1954). Moreover, all grain-size data were entered in GRADISTAT 4.0 (Blott & Pye, 2012) and analysed using statistical formulae following the Method of Moments in Microsoft Visual Basic programming language (i.e. mean grain diameter, sorting, skewness and kurtosis). Grain-size parameters were calculated geometrically (in microns) and logarithmically (using the phi scale) following Krumbein & Pettijohn (1938). Although statistical parameters such as sorting, skewness and kurtosis were deemed useful for distinguishing between sands from beach, dune and aeolian environments (Mason & Folk, 1958) and have been previously used for palaeoenvironmental interpretations (Krumbein & Pettijohn, 1938; Folk & Ward, 1957; Martins, 1965), their applicability is limited in the rock record, where grain disaggregation and sieve analysis are often not feasible. If recorded, sorting indicates the uniformity of grain-size distribution, skewness shows the departure from a symmetry in grain-size distribution, while graphic kurtosis reflects its sharpness or peakedness. If addressed qualitatively in the rock and sedimentary record, poor sorting can help indicate immature sediments, short sediment transport paths and fluctuations in the hydrodynamic energy conditions of the depositional environment (Sahu, 1964). Recorded positive or fine skewness (symmetrical to fine; Blott & Pye, 2012) would indicate the addition of fine-grained material to the predominant coarser-grained fraction, where fines are not removed by currents or waves (under the assumption of minimal sediment mixing). Additionally, positive skewness would characterize unidirectional transport in rivers, which is the case here (Martins, 1965). Meso- to leptokurtic grain-size distribution would indicate slightly better sorting in the central portion of the grain-size distribution than that in the tail (Folk, 1966; Boggs, 2009).

High-resolution CT scanning was carried out on a GEOTEK MSCL-XCT to visualize sedimentary and biogenic structures, biogenic tiering and the nature of bed contacts within whole cores. The scanned cores were slabbed using a circular table saw (model ETS 3151 L Sawking), logged, photographed in daylight and sampled every 3 cm.

The organic matter content of the samples was established using the loss-on-ignition (LOI) technique outlined by Heiri *et al.* (2001). Wet sediment samples were desiccated by baking at 105°C for 24 to 25 h, and the initial weight of the dry samples was measured. The samples were then calcinated for 2 to 4 h at 550°C to remove any trace of organics, and the final mass of the sediment was measured. The difference between the initial and final weight was calculated in percentages, quantifying the content of organic matter in the sample.

The calcium carbonate content was estimated using a calcimeter Eijkelkamp following the Scheibler method modelled after Kretzschmar (1991) and based on a volumetric technique by adding hydrochloric acid to the sample. The difference in water levels measured in a burette is an indication of the released quantity of CO_2, from which the carbonate content is calculated. The carbonate content is expressed as an equivalent calcium carbonate content. The results of the grain size, organic matter and calcium carbonate content analyses are presented in Tables 1 and 3.

The 3D volume created by CT was cut vertically at 0° to 180° and 270° to 90° to produce core slices. CT image reconstruction for the five cores was performed using Geotek Reconstructor software. Geotek CT_Quickview software was utilized to obtain representative down-core orthogonal slices from core segments. All core slices were then analysed in terms of neoichnological assemblages, tiering relationships, degree of bioturbation, potential originating organisms, taphonomic potential and physical sedimentary structures. The degree of plane-bedding and cross-section bioturbation was determined using the bioturbation index (BI)—a semi-quantitative assessment of bioturbation intensity based on the percentage grades of sediment reworked by organism activity, where BI 0 indicates no bioturbation recorded and all original sedimentary structures preserved, to BI 6, meaning that bedding is totally homogenized by biogenic activity (Reineck (1963) as modified by Taylor & Goldring (1993)).

Statistics on open burrow density from tidal flats were acquired using ImageJ—a public-domain Java image processing and analysis program. Twenty-two areas representing three sites in the middle estuary and two sites in the lower estuary (Fig. 1, Table 2) were chosen for digital image analysis. Two other sites in the lower estuary were excluded from the digital analysis because one of the sites is densely covered by *Zostera noltii*, obscuring the burrows from view, while another site (marsh) contains only large crab burrows, which were excluded from the digital burrow analysis.

Depending on the quality of the collected images, the size of the analysed areas ranged from 100 to 1600 cm^2, with the following parameters collected: generalized burrow counts (open burrows only), burrow density (per m^2), total burrowed area (%) and minimum and maximum burrow diameter (cm). For the image digital analysis, the biogenic structures were grouped together without considering the surrounding disturbed sediments with surficial tracks and traces, and the plane-bedding BI was calculated solely based on open burrow openings. The results are presented in Table 2.

Herein, all biogenic structures made by infauna are named based on their resemblance to known ichnotaxa and established tracemaker-ichnotaxa associations (see Dashtgard, 2011a and references therein). It should be noted that even though modern traces should not be formally named after ichnotaxa (Bertling *et al.*, 2006, 2022), this approach is employed in neoichnology for clarity and consistency (Dashtgard, 2011a).

RESULTS

Grain-size distribution, and organic and calcium carbonate content

Surficial samples: Lateral sediment distribution

The results of grain-size analysis of grab samples and the uppermost layer (0 to 1 cm) of push cores are presented in Table 1 along with statistics (i.e. mean, sorting or standard deviation, skewness and kurtosis). Visual representation of sediment grain-size distributions for all samples along the middle and lower reaches of the Mira River estuary is depicted in Fig. 2. Two ternary diagrams (i.e. gravel-sand-mud and sand-silt-clay) after Folk (1954) with sample allocations are presented in Fig. 3.

In general, the Mira River middle estuary tidal flats (CBr; Table 1) are characterized by silty sand (~6% clay), sandy silt (~23% clay), silt (~23% clay) and slightly gravelly muddy sand (~6% clay), with a deeper, more compact layer sampled by push cores characterized by mud and sandy mud (Table 3). All sediments are poorly to very poorly sorted, and the grain-size distribution is symmetrical to very fine skewed (i.e. shows an excess of fine particles). The sediments are predominantly meso- to leptokurtic. The organic matter content averages 7.2%, with a maximum value of 9.1% and a minimum value of 4.5%. Calcium carbonate values are low, varying between 0% and 2.8%, with an average of 1.6%.

The lower Mira River estuary tidal flats (VNMF) are coarser-grained, being characterized by gravel-bearing medium- to coarse-grained

Table 1. Results of grain size, organic matter and calcium carbonate content analyses for surficial grab sediment and uppermost push core samples.

Site	Site	Sample #	% Pebble	% Granule	% vc Sand	% c Sand	% m Sand	% f Sand	% vf Sand	% Silt	% Clay	Mean, μm/φ	Mean grain size	Sorting (log)	Verbal sorting	Skewness (log)	Verbal skewness	Kurtosis (log)	Verbal kurtosis	Classification	TOC	$CaCO_3$
Casa Branca (CBr)	Site 1	M 1.1	0	0.58	2.83	9.42	16.88	20.38	27.32	16.09	6.50	263/3.3	Medium sand	2.28	Very poorly	0.83	Fine skewed	3.42	Mesokurtic	Silty sand	9.1	2
		M 1.2	0	0	1.13	3.41	13.59	29.08	39.33	9.55	3.91	188/3.2	Fine sand	1.74	Poorly	1.39	Very fine skewed	5.87	Leptokurtic	Silty sand	7.2	1.6
		M 1.3	0.37	2.47	2.86	15.69	15.19	27.96	17.09	12.53	5.84	364/2.8	Medium sand	2.34	Very poorly	0.95	Fine skewed	3.78	Leptokurtic	Slightly gravelly muddy sand	7.9	0
	Site 2	M 1.4	0	0.9	2.28	21.36	16.14	16.33	22.35	14.65	5.99	338/2.9	Medium sand	2.39	Very poorly	0.9	Fine skewed	3.33	Leptokurtic	Silty sand	7.9	1.2
	Site 3	M 1.5	0.33	0.19	0.22	2.98	5.88	32.8	31.71	18.66	7.23	151/3.8	Fine sand	2.05	Very poorly	1.04	Fine skewed	3.75	Leptokurtic	Silty sand	7.5	1.8
		CBR1T.F	0	0	0	0	0.29	3.77	11.12	60.85	23.97	38/6.3	Very coarse silt	1.8	Poorly	0.02	Symmetrical	2.67	Mesokurtic	Sandy silt	4.5	1.7
		CBR2T.F	0	0	0	0	0.24	1.54	8.4	66.20	23.62	33/6.4	Very coarse silt	1.63	Poorly	0.18	Symmetrical	2.94	Mesokurtic	Silt	6.5	2.8
Vila Nova de Milfontes (VNMF)	Site 1	M 2.1	3.11	3.5	10	12.19	23.26	21.13	14.01	10.71	2.09	490/2.2	Medium sand	2.14	Very poorly	0.87	Fine skewed	3.92	Leptokurtic	Gravelly sand	3.6	4.3
		M 2.2	14.91	12.79	11.42	10.79	11.34	7.48	12.2	15.87	3.20	709/1.8	Coarse sand	2.73	Very poorly	0.8	Fine skewed	2.74	Mesokurtic	Gravelly sand	6.4	8.7
	Site 3	M 2.3	0.23	0.24	0.3	3.77	43.4	40.73	8.53	2.40	0.39	287/2.2	Medium sand	1.04	Poorly	2.04	Very fine skewed	12.56	Very leptokurtic	Sand	3.0	35.9
		M 2.4	0.8	1.12	1.39	5.19	21.85	20.14	22.07	21.53	5.91	241/3.4	Fine sand	2.29	Very poorly	0.69	Fine skewed	3.05	Mesokurtic	Slightly gravelly muddy sand	9.5	20.4
	Site 4	M 2.5	0.94	9.68	11.52	14.83	14.72	8.68	16.94	18.05	4.64	668/2.4	Coarse sand	2.78	Very poorly	0.56	Fine skewed	2.55	Mesokurtic	Gravelly muddy sand	7.2	8.1
	Site 2	PVNMF 1	0	0	0.01	0.6	2.85	8.49	16.93	50.42	20.70	62/5.7	Very coarse silt	2.14	Very poorly	−0.05	Symmetrical	2.35	Platykurtic	Sandy silt	6.5	13.8
	Site 3	PVNMF 2	0	0	0.36	7.3	24.7	25.55	12.78	20.47	8.84	208/3.5	Fine sand	2.42	Very poorly	0.94	Fine skewed	2.86	Mesokurtic	Silty sand	2.5	37.4
		PVNMF 3	0	0	1.97	19.45	29.07	20.55	9.74	12.78	6.44	318/2.7	Medium sand	2.35	Very poorly	1.33	Very fine skewed	3.97	Leptokurtic	Silty sand	3.5	38

Table 2. Compilation of physical field measurements (in green), averaged laboratory analyses (in blue), including averaged values for grain size, organic matter and calcium carbonate content analyses, burrow statistics calculated in ImageJ (in grey), and observed biogenic structures and infaunal organisms (in yellow) from two study locales: Casa Branca (CBr) and Vila Nova de Milfontes (VNMF). Note that Sites 2 and 4 of the VNMF are not included in Table 2. Site 2 is densely covered by *Zostera noltii*, obscuring the burrows from view, while Site 4 contains only large crab burrows, which were excluded from the digital burrow analysis.

Site	pH	Sal, ‰	T, °C	O2, %	$CaCO_3$		TOC	Gravel >2 mm	Sand 0.063 –2 mm	Mud >0.063 mm	Lithology	Total burrow area, %	Burrow counts/ m_2	Min trace diameter, mm	Max trace diameter, mm	Trace diameter, mm	Traces and inferred tracemakers
Casa Branca (CBR)	LT: 7.7	LT 24.7	LT: 24.6	LT: 89.4	Site 1	1.6	7.9	0.6	78.8	18.4	Silty sand	0.8	4250	1.2	*2.0	*1–3; 30–50	*Skolithos* (*S. plana, H. diversicolor*), *Planolites* (*H. diversicolor*); *Psilonichnus, Thalassinoides, Spongeliomorpha, Coenobichnus*, scratch marks (*C. maenas*); mottling; cryptic; *Taenidium* (insects)
					Site 2	1.2	7.9	0.9	78.5	20.6	Silty sand	1.3	6700	1.4	*2.0	*1–3; ~10	*Skolithos* (*S. plana/H. diversicolor*), *Polykladichnus*, *Planolites* (*H. diversicolor*); *Arenicolites/Diplocraterion* (*C. carinata*); *Psilonichnus, Thalassinoides, Spongeliomorpha, Coenobichnus*, scratch marks (*C. maenas*); rhizoliths; mottling; cryptic
	↑ HT: 8.0	↑ HT: 28.9	↓ HT: 23.9	↓ HT: 77.6	Site 3	1.8	7.5	0.5	73.6	25.9	Sandy silt and silt	4.1	6500	2.0	*3.5	*3–5; 10–60	*Skolithos, Polykladichnus, Planolites, Palaeophycus* (*H. diversicolor, S. plana*); *Scalinichnus, Siphonichnus, Lockeia*, fugichnia, equilibrichnia (*S. plana*); *Arenicolites/Diplocraterion* (*C. carinata*); *Psilonichnus, Thalassinoides, Spongeliomorpha, Coenobichnus*, scratch marks (*C. maenas*); rhizoliths; mottling; cryptic
Vila Nova de Milfontes (VNMF)	LT: 8.1	LT 35.0	LT: 21.8	LT: 63.5	Site 1	6.5	5.0	17.2	66.9	15.9	Gravelly sand	1.4	3138	2.1	*3.6	*1–10; 20	*Siphonichnus, Scalinichnus, Lockeia*, fugichnia, equilibrichnia (*C. edule, A. alba/S. strictus*?); *Arenicolites/ Diplocraterion* (*C. orientale/C. crangon*?, *C. carinata*, nemertians, *A. marina*); *Curvolithus, Cochlichnus* (gastropods); *Skolithos, Polykladichnus, Planolites* (*H. diversicolor; C. capitata?, C. orientale, C. carinata, B. redeki, A. romijni*); *Psilonichnus* (*C. maenas*); *Archaeonassa/ Taphrhelminthopsis?* (gastropods); mottling; cryptic
	↑ HT: 8.2	↑ HT: 35.3	↓ HT: 17.0	↑ HT: 63.9	Site 3	20.4	7.2	1.9	70.6	22.7	Sand, sandy silt, silty sand	1.4	1550	2.6	*4.7	*1–8; 10	*Siphonichnus, Scalinichnus, Lockeia*, fugichnia, equilibrichnia (*C. edule, S. plana*); *Arenicolites/Diplocraterion, Skolithos, Polykladichnus, Planolites, Palaeophycus* (*H. diversicolor, C. capitata?, C. orientale/C. crangon*?); agglutinated *Skolithos, Polykladichnus, Arenicolites/Diplocraterion* (*A. marina, P. kereni*); *Ophiomorpha* (amphipods); *Psilonichnus* (*C. maenas*); *Archaeonassa/ Taphrhelminthopsis?* (gastropods); rhizoliths; mottling; cryptic

*Max trace diameter excluding crab burrows; Max trace diameter including crab burrows. LT, low tide; HT, High tide; ↓, Decreasing trend; ↑, Increasing trend. Green, Field measurements; Blue, Laboratory measurements; Grey, ImageJ analysis; Yellow, Field observations.

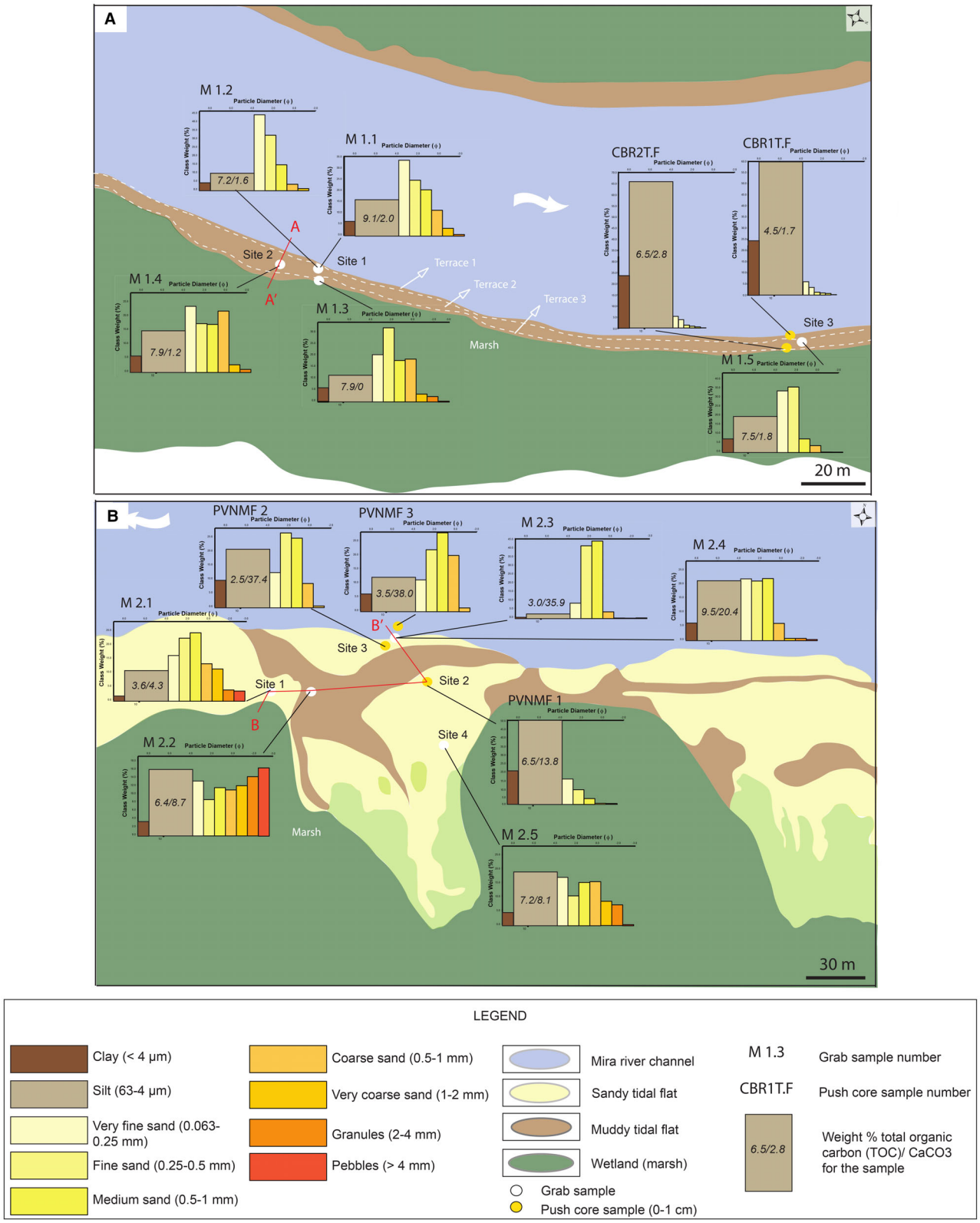

Fig. 2. Map of sediment distribution (surficial grab samples) and upper layer of push cores across the tidal flats of the middle (A) and lower (B) Mira River estuary with site and sample numbers. Middle estuary (A) also depicts the subdivision of the tidal flats into three terraces corresponding to lower, middle, and upper tidal flats. Red lines represent cross-sections along and across the tidal flats depicted in Fig. 13.

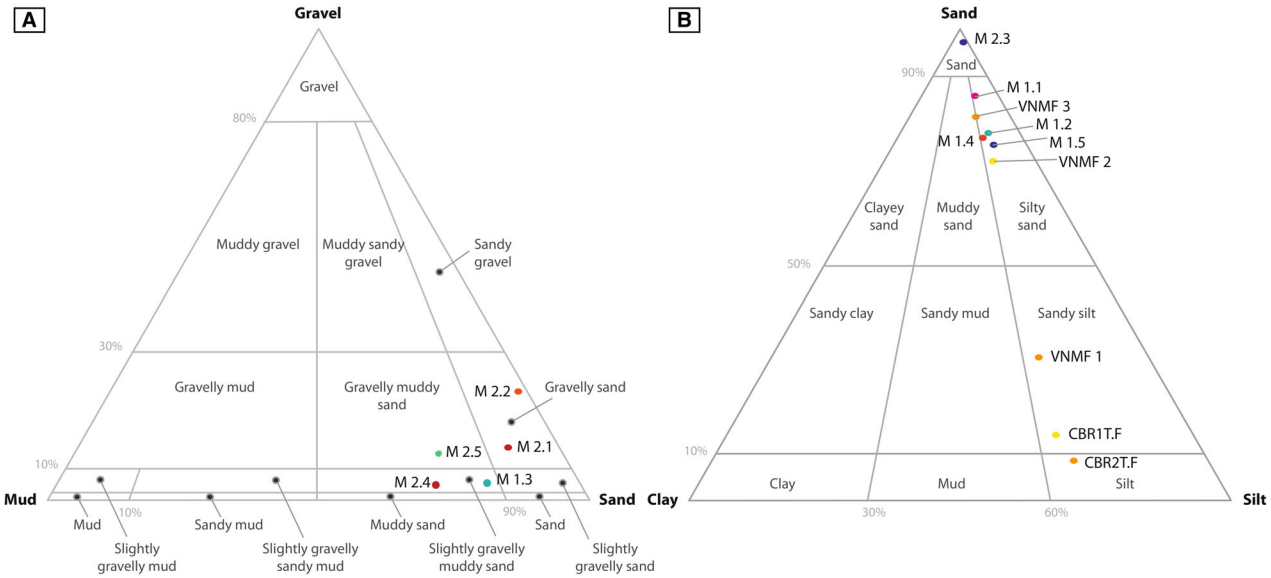

Fig. 3. Ternary diagrams for gravel-sand-mud (A) and sand-silt-clay (B) distribution for the Mira River estuary grab and uppermost layer of push core samples (after Folk, 1954).

sand and gravel-bearing muddy sand deposited on the upper tidal flat. By contrast, the middle to lower portions of the VNMF tidal flats present sandy silt, silty fine- to medium-grained sand and medium-grained sand. Sediment sorting is generally very poor, with skewness ranging from very fine (i.e. excess of fine particles) to symmetrical. With respect to kurtosis, the sediments vary from platykurtic to very leptokurtic. The tidal flats of the lower Mira River estuary present semi-detached sand bars oriented parallel to the shore (Fig. 4B, D) with lower areas occupied by tidal creeks and tidal flats covered in microscopic algae, *Spartina maritima*, and *Zostera noltii* during spring–summer seasons (Fig. 4D). Organic matter content averages 5.3%, with a maximum of 9.5% and a minimum of 2.5%. Calcium carbonate content is high, averaging 20.8%, with a maximum value reaching 38% in the lower tidal flat and a minimum of 4.3% in the upper tidal flat.

Push cores: Vertical sediment distribution

Results of grain-size analysis of the vertical push cores (sampling step of 3 cm) are presented in Table 3 along with sample statistics. The ternary diagrams (sand-silt-clay) after Folk (1954) and grain-size distribution diagrams with sample allocation are presented in Fig. 5.

In general, the Mira River middle estuary push cores (CBR1T.F and CBR2T.F) are represented by very fine-grained sediments, predominantly mud (silt+clay >90%) and sandy mud (silt+clay 79.5 to 90%). Silt is always the predominant component compared to clay, ranging from 64.9% to 77.8% for CBR1T.F and from 60.4% to 80.0% for CBR2T.F. Clay percentages are similar in both cores, constituting an average of 18.1% for CBR1T.F and 20.7% for CBR2T.F. Sand percentages never exceed 20.5% in CBR1T.F and 12.9% in CB2T.F. In both cores, the sediments are poorly sorted, except for CBR1T.F at a depth of 6 to 7 cm (very poorly sorted and symmetrically skewed) and CBR2T.F at depths of 6 to 7 cm and 45 to 46 cm (coarsely skewed). The sediments of these push cores are also predominantly mesokurtic and less commonly platykurtic, except for a leptokurtic layer at a depth of 6 to 7 cm in CBR2T.F. The organic matter content is slightly higher in CBR1T.F, ranging from 4.5% to 12.9%, although the averages in both cores are similar (7.1 to 7.2%). Calcium carbonate content is also very similar in both cores, with a maximum of 4.3% for CBR1T.F and 4.1% for CBR2T.F.

In the lower Mira River estuary tidal flats (push cores VNMF1–3), the sediments are coarser and constitute predominantly sandy mud (VNMF1, VNMF2 and VNMF3), followed by muddy sand (VNMF2 and VNMF3) and slightly gravelly muddy sand (VNMF2). VNMF1 is the finest (with a mud layer located

Table 3. Results of grain-size analysis of vertical push cores (sampling step of 3 cm) and sample statistics.

Site #	Sample #	% Pebble	% Granule	% vc Sand	% c Sand	% m Sand	% f Sand	% vf Sand	% Silt	% Clay	Mean, μm/φ	Mean grain size	Sorting (log)	Verbal sorting	Skewness (log)	Verbal skewness	Kurtosis (log)	Verbal kurtosis	Classification	TOC	$CaCO_3$
CBR1T.F	0–1 cm	0	0	0	0	0.3	3.8	11.3	79.2	16.0	15.5/6.0	Coarse Silt	1.84	Poorly	0.11	Symmetrical	2.37	Platykurtic	Sandy Mud	4.5	1.7
	3–4 cm	0	0	0	0	0.5	1.1	5.6	86.3	20.1	11.3/6.5	Medium Silt	1.69	Poorly	−0.09	Symmetrical	2.73	Mesokurtic	Mud	6.5	0.5
	6–7 cm	0	0	0	1.8	2.6	4	12	74.3	16.5	17.8/5.8	Coarse Silt	2.08	Very poorly	−0.24	Symmetrical	2.67	Mesokurtic	Sandy Mud	6.9	1.2
	9–10 cm	0	0	0	0	0.6	2.9	11	79.9	16.4	15.1/6	Medium Silt	1.83	Poorly	0.10	Symmetrical	2.40	Platykurtic	Sandy Mud	12.9	1.5
	12–13 cm	0	0	0	0	0.6	3	9.8	81.3	1.7	14.3/6.1	Medium Silt	1.81	Poorly	−0.02	Symmetrical	2.46	Platykurtic	Sandy Mud	7.0	1.5
	15–16 cm	0	0	0	0.1	0,7	1.5	5.6	85.2	21.6	10.7/6.5	Medium Silt	1.73	Poorly	−0.25	Symmetrical	2.85	Mesokurtic	Mud	7.0	2.1
	18–19 cm	0	0	0	0.3	1	1.1	3.9	87.8	20.2	11.4/6.4	Medium Silt	1.66	Poorly	−0.25	Symmetrical	3.40	Mesokurtic	Mud	8.4	1.5
	21–22 cm	0	0	0	0	0	0.4	2.6	90.1	21.1	9.8/6.7	Medium Silt	1.51	Poorly	0.13	Symmetrical	2.65	Mesokurtic	Mud	6.5	1.1
	24–25 cm	0	0	0	0	0.6	0.9	4.3	88.5	19.0	11.7/6.4	Medium Silt	1.61	Poorly	0.02	Symmetrical	2.93	Mesokurtic	Mud	8.0	4.3
	27–28 cm	0	0	0	0.1	0.2	1.2	6.8	83.2	23.2	9.6/6.7	Medium Silt	1.78	Poorly	−0.29	Symmetrical	2.54	Platykurtic	Mud	6.5	3.4
	30–31 cm	0	0	0	0.2	0.8	1.9	7.3	82.5	21.1	11.3/6.5	Medium Silt	1.83	Poorly	−0.26	Symmetrical	2.72	Mesokurtic	Sandy Mud	6.9	1.3
	33–34 cm	0	0	0	0.1	0.9	1.6	5.9	85.1	21.6	11.2/6.5	Medium Silt	1.70	Poorly	−0.31	Symmetrical	3.20	Mesokurtic	Mud	5.5	0.1
CBR2T.F	0–1 cm	0	0	0	0	0.2	1.5	8.6	84	5.6	14.5/6.1	Medium Silt	1.72	Poorly	0.25	Symmetrical	2.530	Platykurtic	Sandy Mud	6.5	2.8
	3–4 cm	0	0	0	0.3	2	2.8	7.7	78.9	8.3	11.8/6.4	Medium Silt	1.99	Poorly	−0.32	Symmetrical	2.737	Mesokurtic	Sandy Mud	7.0	1.9
	6–7 cm	0	0	0.2	1.9	1.3	1.2	3.1	82.3	10.2	8.5/6.9	Medium Silt	1.95	Poorly	−0.99	Coarse	4.542	Leptokurtic	Mud	6.0	1.1
	9–10 cm	0	0	0	0.2	1.3	1.8	6.3	84.4	6	12.5/6.3	Medium Silt	1.77	Poorly	−0.24	Symmetrical	3.050	Mesokurtic	Mud	6.5	1.5
	12–13 cm	0	0	0	9	9.7	1	5.3	87.3	5.8	12.7/6.3	Medium Silt	1.66	Poorly	0.06	Symmetrical	2.864	Mesokurtic	Mud	8.0	2.0
	15–16 cm	0	0	0	0	0.8	0.9	3.8	88.8	5.7	12.1/6.4	Medium Silt	1.59	Poorly	0.03	Symmetrical	3.181	Mesokurtic	Mud	6.0	2.8
	18–19 cm	0	0	0	0	0.1	0.5	4.4	89.7	5.3	12.7/6.3	Medium Silt	1.56	Poorly	0.29	Symmetrical	2.671	Mesokurtic	Mud	6.5	3.0
	21–22 cm	0	0	0	0.1	0.8	0.9	5.5	85.6	7.2	10.9/6.5	Medium Silt	1.73	Poorly	−0.16	Symmetrical	2.838	Mesokurtic	Mud	6.0	2.1
	24–25 cm	0	0	0	0	0.7	1.1	5	87.6	5.6	12.7/6.3	Medium Silt	1.64	Poorly	0.05	Symmetrical	2.937	Mesokurtic	Mud	9.9	4.1
	27–28 cm	0	0	0	0.1	0.5	0.8	5	86.7	7	10.5/6.6	Medium Silt	1.67	Poorly	−0.13	Symmetrical	2.821	Mesokurtic	Mud	7.0	2.3
	30–31 cm	0	0	0	0.5	0.7	0.2	3.1	87	8.5	9.4/6.7	Medium Silt	1.71	Poorly	−0.34	Symmetrical	3.378	Mesokurtic	Mud	7.4	3.4
	33-34 cm	0	0	0	0	0.3	0.7	7.5	84.9	6.6	12.8/6.3	Medium Silt	1.73	Poorly	0.17	Symmetrical	2.430	Platykurtic	Mud	6.5	2.6
	36–37 cm	0	0	0	0	0.9	2	10.1	80.9	6.2	14/6.2	Medium Silt	1.84	Poorly	0.04	Symmetrical	2.443	Platykurtic	Sandy Mud	7.4	2.9
	39–40 cm	0	0	0	0	0	0.3	2.7	89.4	7.6	9.3/6.8	Medium Silt	1.51	Poorly	0.09	Symmetrical	2.672	Mesokurtic	Mud	8.0	1.6
	42–43 cm	0	0	0	0	0	0.6	2.8	85.6	11	6.8/7.2	Fine Silt	1.54	Poorly	−0.39	Symmetrical	3.001	Mesokurtic	Mud	9.0	2.5
	45–46 cm	0	0	0	0	0	0.6	2.6	83	13.9	6.0/7.4	Fine Silt	1.56	Poorly	−0.46	Coarse	3.149	Mesokurtic	Mud	5.5	3.1
VNMF 1	0–1 cm	0	0	0	0.6	2.8	8.5	17.1	66.6	4.4	22.2/5.5	Coarse Silt	2.11	Very poorly	0.08	Symmetrical	2.22	Platykurtic	Sandy Mud	6.5	13.8
	3–4 cm	0	0	0	1.5	5.6	12.4	20.4	56.3	3.8	31.2/5	vc Silt	2.23	Very poorly	0.28	Symmetrical	2.22	Platykurtic	Sandy Mud	5.0	17.9
	6–7 cm	0	0	0	0.4	3.3	9.4	17.2	66	3.6	24.8/5.3	Coarse Silt	2.05	Very poorly	0.14	Symmetrical	2.30	Platykurtic	Sandy Mud	6.5	19.8
	9–10 cm	0	0	0	0.5	2.6	6.5	13.3	72.7	4.4	19.2/5.7	Coarse Silt	2.03	Very poorly	−0.08	Symmetrical	2.40	Platykurtic	Sandy Mud	6.5	17.3
	12–13 cm	0	0	0	0.8	3.1	6.6	14.5	69.9	5	19.7/5.7	Coarse Silt	2.12	Very poorly	−0.05	Symmetrical	2.31	Platykurtic	Sandy Mud	6.0	15.1
	15–16 cm	0	0	0	1.1	4	6.2	13.2	71.5	4.1	21.9/5.5	Coarse Silt	2.06	Very poorly	−0.05	Symmetrical	2.50	Platykurtic	Sandy Mud	8.5	14.3
	18–19 cm	0	0	0	0.6	3.4	6.9	13	71.5	4.6	19/5.7	Coarse Silt	2.10	Very poorly	−0.14	Symmetrical	2.33	Platykurtic	Sandy Mud	5.4	19.0
	21–22 cm	0	0	0	0.3	3.1	6.5	13	71.4	5.7	17.2/5.9	Coarse Silt	2.13	Very poorly	−0.13	Symmetrical	2.22	Platykurtic	Sandy Mud	5.0	16.0
	24–25 cm	0	0	0	0	0.8	3.1	8.6	81.8	5.6	13.3/6.2	Medium Silt	1.81	Poorly	−0.15	Symmetrical	2.58	Mesokurtic	Sandy Mud	5.5	10.1
	27–28 cm	0	0	0	0	1	2.5	8	82.8	5.7	13.5/6.2	Medium Silt	1.79	Poorly	−0.05	Symmetrical	2.66	Mesokurtic	Sandy Mud	6.5	10.2
	30–31 cm	0	0	0	0.1	0.9	1.3	5.9	86.6	5.2	12.9/6.3	Medium Silt	1.68	Poorly	−0.07	Symmetrical	2.95	Mesokurtic	Mud	6.0	7.1
	33–34 cm	0	0	0	0.1	1.2	3.4	10.1	78.5	6.8	13.9/6.2	Medium Silt	1.93	Poorly	−0.07	Symmetrical	2.44	Platykurtic	Sandy Mud	6.5	8.8
VNMF 2	0–1 cm	0	0	0.4	7.3	24.7	25.6	12.9	27.3	1.9	95.1/3.4	vf Sand	2.30	Very poorly	1.01	Symmetrical	3.105	Mesokurtic	Muddy Sand	2.5	37.4
	3–4 cm	0	0	0.4	6.2	21.7	26.1	17.4	26.9	1.4	97.3/3.4	vf Sand	2.10	Very poorly	1.03	Symmetrical	3.509	Mesokurtic	Slightly Gravelly Muddy Sand	2.5	35.3
	6–7 cm	0	0	0	1.8	11.2	18.9	20.9	44.9	2.2	51.7/4.3	vc Silt	2.13	Very poorly	0.60	Symmetrical	2.624	Mesokurtic	Muddy Sand	5.0	29.2
	9–10 cm	0	0	0.1	2.9	7.9	16.3	20.2	49.4	3.1	42/4/6	vc Silt	2.25	Very poorly	0.41	Very fine	2.411	Platykurtic	Sandy Mud	7.5	16.8
	12–13 cm	0	0	0	1.1	9.2	16.9	19.5	50	3.3	38.6/4.7	vc Silt	2.28	Very poorly	0.42	Very fine	2.195	Platykurtic	Sandy Mud	5.0	27.5

Table 3. (continued)

Site #	Sample #	% Pebble	% Granule	% vc Sand	% c Sand	% m Sand	% f Sand	% vf Sand	% Silt	% Clay	Mean, μm/φ	Mean grain size	Sorting (log)	Verbal sorting	Skewness (log)	Verbal skewness	Kurtosis (log)	Verbal kurtosis	Classification	TOC	$CaCO_3$
	15–16 cm	0	0	0	0.1	2.2	5	9.3	78.5	4.9	15.9/6	Coarse Silt	1.91	Poorly	−0.18	Symmetrical	2.667	Mesokurtic	Sandy Mud	4.5	19.0
	18–19 cm	0	0	0	0.5	4.7	8.4	13.6	67.4	5.4	20.5/5.6	Coarse Silt	2.21	Very poorly	−0.04	Symmetrical	2.182	Platykurtic	Sandy Mud	7.5	22.3
	21–22 cm	0	0	0	0.7	4.5	9.8	15.9	64.9	4.2	24.2/5.4	Coarse Silt	2.16	Very poorly	0.08	Symmetrical	2.216	Platykurtic	Sandy Mud	5.0	20.5
	24–25 cm	0	0	0	0.6	3.2	6.3	12.6	72.8	4.5	19.8/5.7	Coarse Silt	2.03	Very poorly	−0.06	Symmetrical	2.489	Platykurtic	Sandy Mud	5.0	16.5
	27–28 cm	0	0	0	1.3	6.7	13.2	16	58.5	4.3	29.1/5/1	Coarse Silt	2.29	Very poorly	0.16	Symmetrical	2.129	Platykurtic	Sandy Mud	4.0	19.5
	30–31 cm	0	0	0	0.3	2.8	6.1	11.2	73.4	6.2	15.6/6	Coarse Silt	2.10	Very poorly	−0.22	Symmetrical	2.350	Platykurtic	Sandy Mud	6.4	14.6
	33–34 cm	0	0	0	0.5	1.7	2.9	8	77.2	9.6	10.5/6.6	Medium Silt	2.05	Very poorly	−0.49	Coarse	2.688	Mesokurtic	Sandy Mud	5.0	14.8
	36–37 cm	0	0	2	14.5	13.4	9,6	10.8	463	3.5	55.4/4.2	vc Silt	2.79	Very poorly	0.20	Symmetrical	1.876	Platykurtic	Slightly Gravelly Muddy Sand	2.5	29.7
	39–40 cm	0	0	2.2	19.9	19.8	14	12.2	30.4	1.5	112.8/3.1	vf Sand	2.45	Very poorly	0.74	Very fine	2.622	Mesokurtic	Muddy Sand	3.0	26.3
	42–43 cm	0	0	3.5	27.7	22.7	10.2	8.8	25.2	1.8	143.9/2.8	Fine Sand	2.60	Very poorly	0.99	Symmetrical	2.862	Mesokurtic	Muddy Sand	3.5	32.1
VNMF 3	0–1 cm	0	0	2	19.5	29.1	20.6	9.8	17.7	1.5	159.8/2.6	Fine Sand	2.25	Very poorly	1.37	Very fine	4.24	Leptokurtic	Muddy Sand	3.5	38.0
	3–4 cm	0	0	2.6	19.4	31.8	24.4	9.1	12	0.8	202.9/2.3	Fine Sand	1.90	Poorly	1.67	Very fine	5.97	Leptokurtic	Muddy Sand	3.5	39.5
	6–7 cm	0	0	0.1	5.2	12.4	11.2	9.5	55.6	6.1	29/5.1	Coarse Silt	2.71	Very poorly	−0.05	Symmetrical	1.82	Platykurtic	Sandy Mud	2.5	26.5
	9–10 cm	0	0	0	0.5	4.3	5.7	8.3	74.5	6.7	14.2/6.1	Medium Silt	2.17	Very poorly	−0.42	Symmetrical	2.51	Platykurtic	Sandy Mud	4.0	29.1
	12–13 cm	0	0	0	2.9	9.4	9.9	9.9	62.5	5.4	23.9/5.4	Coarse Silt	2.50	Very poorly	−0.18	Symmetrical	1.99	Platykurtic	Sandy Mud	5.0	23.2
	15–16 cm	0	0	0	1	4.8	7.2	13.3	69.5	4.2	23.3/5.4	Coarse Silt	2.10	Very poorly	0.01	Symmetrical	2.45	Platykurtic	Sandy Mud	4.0	28.0
	18–19 cm	0	0	0	2.8	9.9	12.7	13.5	55.4	5.8	28/5.2	Coarse Silt	2.56	Very poorly	0.06	Symmetrical	1.88	Platykurtic	Sandy Mud	6.9	23.1
	21–22 cm	0	0	0	0	1.2	3.5	8.5	81.3	5.4	14.1/6.1	Medium Silt	1.83	Poorly	−0.13	Symmetrical	2.65	Leptokurtic	Sandy Mud	5.5	9.2
	24–25 cm	0	0	0	1	4.4	5.8	7.4	70/8	10.6	11.9/6.4	Medium Silt	2.34	Very poorly	−0.53	Coarse	2.49	Platykurtic	Sandy Mud	7.4	10.9
	27–28 cm	0	0	0	0.1	3.1	6.7	12.8	71.3	6	17.8/5.8	Coarse Silt	2.12	Very poorly	−0.03	Symmetrical	2.23	Platykurtic	Sandy Mud	4.0	13.7
	30–31 cm	0	0	0	1.7	4.5	5.6	11.4	70.8	6	18.9/5.7	Coarse Silt	2.21	Very poorly	−0.19	Symmetrical	2.45	Platykurtic	Sandy Mud	3.5	16.4
	33–34 cm	0	0	6.2	47.9	18.4	0.8	3.7	20.7	2.3	215.1/2.2	Fine Sand	2.76	Very poorly	1.35	Very fine	3.43	Leptokurtic	Muddy Sand	1.5	27.5
	36–37 cm	0	0	8.6	58.5	21.7	0.1	1.9	8.4	0.8	418/4/1.3	Coarse Sand	1.90	Poorly	2.67	Very fine	9.64	Very leptokurtic	Sand	0.5	30.3
	39–40 cm	0	0	0	0.1	1	1.8	7.2	82.9	7	12/6.4	Medium Silt	1.82	Poorly	−0.15	Symmetrical	2.68	Mesokurtic	Sandy Mud	3.5	13.4
	42–43 cm	0	0	6.2	56.7	25.8	0.4	2.1	8.2	0.8	399.2/1.3	Coarse Sand	1.89	Poorly	2.68	Very fine	9.69	Very leptokurtic	Sand	3.0	28.9

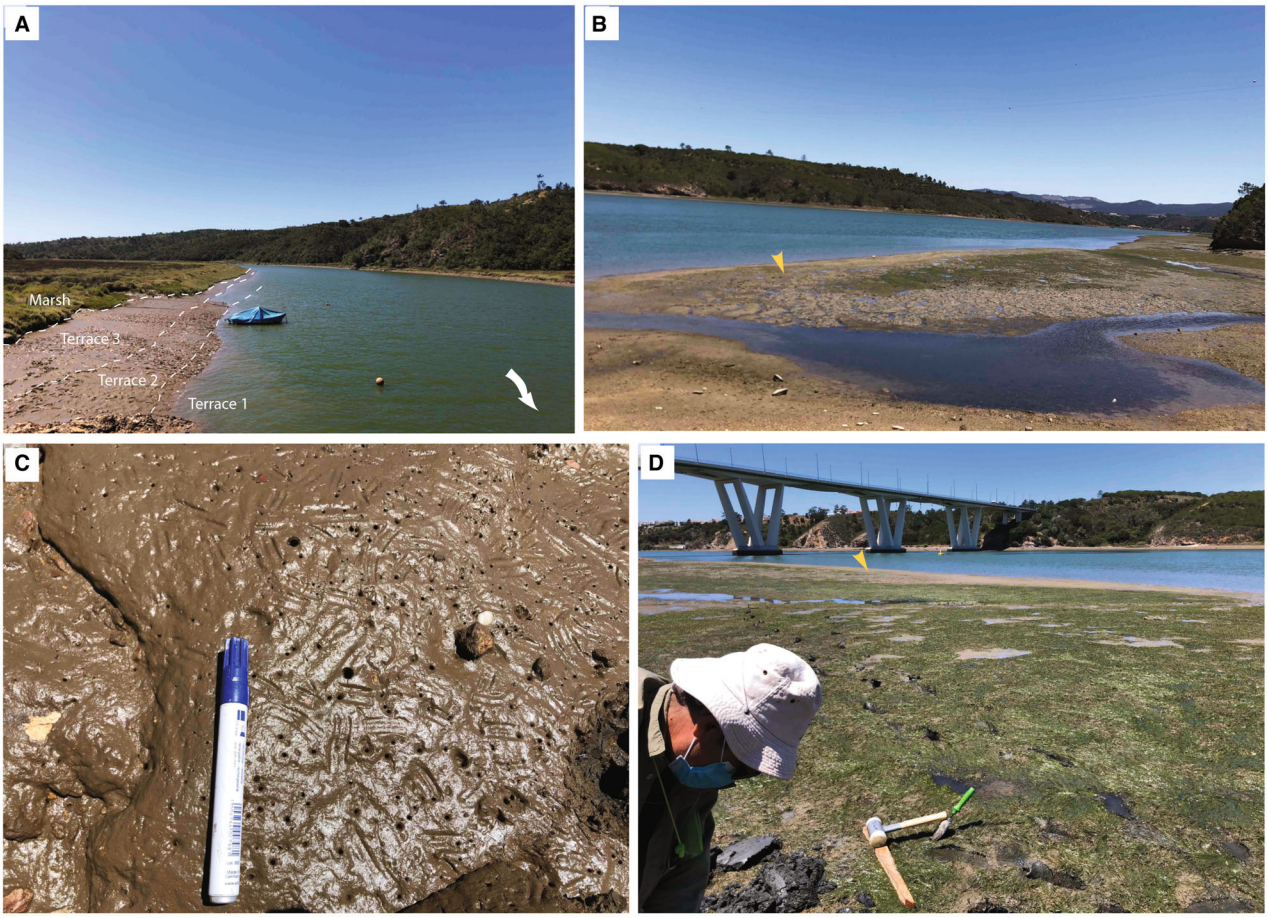

Fig. 4. Geomorphology of the middle (A) and lower (B) Mira estuary tidal flats, with the direction of the fluvial current (white arrow) and semi-detached sand bars (yellow arrow). (C) Semi-consolidated mud on the middle estuary tidal flat is fully covered in crab-generated scratch marks/fish-generated 'cruzianaeform' bite marks, as well as other burrow openings. Pen for scale (1.5 cm in diameter). (D) Lower Mira estuary sandy tidal flats occupied by patches of microscopic algae, *Spartina maritima*, and *Zostera noltii* and semi-detached sand bars in the background (yellow arrow).

at 30 to 31 cm) and VNMF3 is the coarsest, preserving sand layers at the base (36 to 37 cm and 42 to 43 cm). In VNMF1 and VNMF2, mud is the predominant component, reaching 91.8% and 86.9%, respectively. Silt ranges from 49.1% to 76.4% for VNMF1 and from 21.7% to 69.6% for VNMF2. Sand averages 22.1%, 43.3% and 44.6% for the three push cores, respectively. The lower estuary push cores are predominantly very poorly sorted. In the bottom part of VNMF1 and VNMF3 and in a few layers of VNMF2 (15 to 16 cm) and VNMF3 (3 to 4 cm, 21 to 22 cm), the sediments are poorly sorted. The skewness is symmetrical in VNMF1 and predominantly symmetrical with some very finely skewed layers in VNMF2 and VNMF3. Moreover, VNMF3 showcases a coarsely skewed layer at a depth of 24 to 25 cm. In terms of kurtosis, the sediments are platykurtic, except for the lower part of VNMF1 and VNMF2, where mesokurtic sediments are also present. VNMF3 differs from the other cores by showing leptokurtic kurtosis, especially at the top of the core and very leptokurtic sediments at the base of the core (36 to 37 cm and 42 to 43 cm). Organic matter content in the lower estuary push cores (VNMF) is lower than that in the middle estuary ones (CBr). The average values diminish from VNMF1 to VNMF2 and VNMF3, constituting 6.2%, 4.6% and 3.9%, respectively. Inversely, the calcium carbonate content in the lower

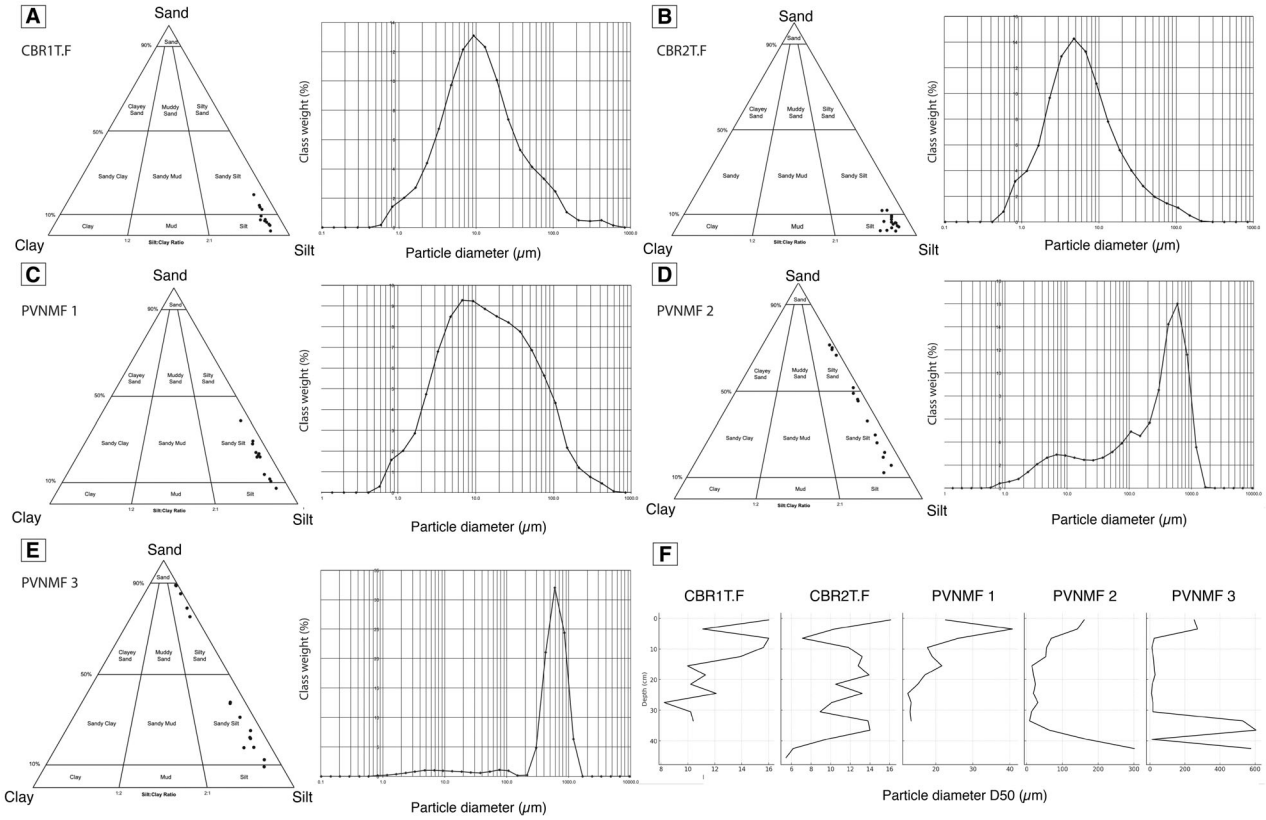

Fig. 5. Ternary diagrams (sand-silt-clay) and grain-size distribution diagrams (with particle diameter in μm) for push cores CBR1T.F (A), CBR2T.F (B), VNMF 1 (C), VNMF 2 (D) and VNMF 3 (E). (F) Variation in grain size (D50) relative to depth for each push core.

estuary cores is much higher than that in the middle estuary, with an average of 14.1% (VNMF1), 24.1% (VNMF2) and 23.8% (VNMF3).

Physico-chemical parameters

Water salinity, temperature and dissolved oxygen concentrations were obtained at the surveyed sites during neap low and high slack-water periods (Table 2), with pH from historical data (see Methods section). At neap low tide (LT) and high tide (HT), the measured salinities in the middle estuary (CBr) were 24.7‰ and 28.9‰, the temperatures were 24.6°C and 23.9°C, and oxygen saturations reached 89.4% and 77.6%, with estimated pH values of 7.7 and 8.0, respectively. As for the lower estuary (VNMF), at neap low and high tides, the salinities were 35.0‰ and 35.3‰, water temperatures were 21.8°C and 17°C, oxygen saturations ranged from 63.5% to 63.9%, and estimated pH values were 8.1 and 8.2, respectively.

Neoichnology

Trace makers and burrow morphology: Field observations

At the middle estuary location (CBr), the depositional surfaces occupying the lower, middle, and upper terraces, as well as the marsh cliffs (Fig. 4A), are characterized by persistent bioturbation (Fig. 6, Table 2). In plan view, the lower and middle intertidal flats are dotted with small burrow openings 1–3 mm and 3–5 mm in diameter (Figs 4C and 6F). In cross-section, however, burrows are predominantly vertical, inclined, Y-shaped or inverse Y-shaped (Fig. 6A to E), branching at a depth of ~5 cm (Fig. 6B). Some burrows present shorter, horizontal components, with the number of horizontal burrows increasing upwards along the tidal flat slope (Fig. 6J). The burrows are lined with mucus within the first ~1 cm of brown, oxygenated mud and are protected by thick brown linings where they pass into dysoxic, black sediments (Fig. 6A to C, E). These burrows penetrate between 1 to 2 cm

and 6 to 7 cm deep and can be classified as *Skolithos, Arenicolites, Diplocraterion, Polykladichnus* and *Palaeophycus* (Table 2). The larger diameter burrows (3 to 5 mm) are attributed to mobile vermiform organisms such as *Hediste diversicolor* (Fig. 6A, B) and *Nephtys caeca*, with the latter being reported as the predominant bioturbator in the Mira mudflats by Costa *et al.* (2001). The smaller burrows (1 to 3 mm in diameter) are likely formed by isopods such as *Cyathura carinata* (Fig. 6C). *Skolithos* and *Arenicolites* can be produced by siphons of bivalves such as *Scrobicularia plana* and *Corbicula fluminea* (Fig. 6E, F). Living shells of *Scrobicularia plana* were discovered ~3 to 10 cm below the substrate surface (Fig. 6E). The soft to semi-consolidated mud surfaces are also abundantly covered in marks formed by crab chelipeds or Sparidae fish (Fig. 4C), locomotion trackways by *Carcinus maenas/Uca tangeri* (Fig. 6H), burrow entrances/exits measuring ~3 to 4 cm in diameter (some with sculptings near the entrance; Fig. 6G) by *Carcinus maenas/Uca tangeri* and elongated faecal pellets (Fig. 6G, H). This array of biogenic structures is produced by the Atlantic shore crab *Carcinus maenas*, fiddler crab *Uca tangeri* and possibly by Sparidae fish (Vinagre *et al.*, 2010; Muñiz *et al.*, 2015; Belaústegui & Muñiz, 2016; Shchepetkina, 2025; Fig. 6G inset). *Carcinus maenas* was observed during the daylight hours roaming the tidal flats and marshes, seeking shelter in burrows, cavities and under rocks. Crab tracks and trackways are similar to *Coenobichnus* (Fig. 6H), scratch marks or fish bite marks are 'cruzianaeform' (Muñiz *et al.*, 2015; Shchepetkina, 2025), open burrows resemble *Psilonichnus* and *Spongeliomorpha* (Shchepetkina, 2025; Fig. 6G), whereas faecal pellets are *Favreina*-like (Shchepetkina, 2025). The sediments can also contain root traces (rhizoliths) and other detrital debris.

The upper tidal flat is represented by more consolidated sediments, commonly covered in desiccation cracks (Fig. 6H, I). The surface exhibits abundant dotted pits (locomotion marks; Fig. 6H) and faecal pellets (Fig. 6G, H) from *Carcinus maenas/Uca tangeri*, horizontal lined burrows (3 to 5 mm in diameter; Fig. 6J) found 2 to 3 cm below the surface (unknown producer), and back-filled excavations with tiny mud pellets, likely formed by an insect or insect larvae (Fig. 6I). The burrow morphologies resemble *Coenobichnus* (tracks and trackways; Fig. 6H), *Palaeophycus* (horizontal burrows; Fig. 6J) and *Taenidium* (back-filled burrows; Fig. 6I). Surfaces located near the marsh cliff contain abundant marsh-eroded mud clasts (Fig. 6K).

Marsh cliffs are 30 to 90 cm in height and consist of semi-consolidated sediment. They contain open *Psilonichnus* (Fig. 6L) approximately 1 to 2 cm and 6 to 7 cm wide, maintained by *Uca tangeri* and probably used as shelter by *Carcinus maenas*. However, most of the burrows seem to be abandoned due to substrate desiccation. Marsh cliffs can also be intensively penetrated by root traces (Fig. 6L). The high marsh sediments contain deep mud cracks and are partially vegetated by *Sarcocornia* sp., *Atriplex* (*Halimione*) *portulacoides, Spartina maritima* and *Sueda maritima*, as well as *Juncus maritimus* and *Limonium narbonense* in more elevated areas (Fig. 6K).

The tidal flats of the VNMF lower estuary exhibit greater variability in morphology, sediment composition and neoichnological signature (Table 2). The lower tidal flat is composed of ~1 cm of brownish sand and contains dysoxic, black sediments beneath (Fig. 7A to C). The tidal flat surface is covered by small openings (1 to 2 mm in diameter) of vertical to inclined burrows (Fig. 7A, B), some with agglutinated linings (~3 mm thick; Fig. 7C), similar to thin *Skolithos* and *Arenicolites* and likely formed by polychaetes (e.g. *Hediste diversicolor*) and the tube-living worm *Lagis koreni* (Fig. 7C inset). Some burrows feature a Fe halo (Fig. 7D, F), extend deeper into the substrate and resemble *Skolithos* and *Palaeophycus*. Other burrows branch out at a depth of 3 to 5 cm, forming horizontal components similar to *Palaeophycus* and *Planolites* (Fig. 7D). The top 1 to 2 cm of the sediment commonly contains U-shaped *Arenicolites* and *Diplocraterion* produced by *Corophium orientale* (Fig. 7E) and Y-shaped burrows similar to *Polykladichnus* likely produced by *Hediste diversicolor* or *Nephtys caeca*. Juvenile *Hediste diversicolor* (Fig. 7B) also seems to produce 2 to 3 mm thick vertical to inclined traces similar to *Skolithos*, whereas *Capitella capitata* (Fig. 7B inset) produces 0.5 to 1 mm thick burrows similar to *Skolithos* and *Palaeophycus*. The producer of larger (7 to 8 mm diameter), mud-lined *Skolithos*-like burrows was not visible. Vertical to inclined *Ophiomorpha* with a knobbly surface is likely the product of decapod activity (Fig. 7F).

The middle portion of the tidal flat is occupied by a tidal creek and covered by gravel, filamentous green algae, *Fucus vesiculosus* and

Rhodophyta (Fig. 7G, H). The upper 1 cm is composed of brownish muddy sand, gravel and seaweed, with the rest being represented by dysoxic, black mud (Fig. 7H, I). The creek is occupied by openings of vertical, thickly lined burrows similar to *Skolithos, Arenicolites* and *Polykladichnus*, as well as larger, vertical to inclined shafts of crabs that could represent *Thalassinoides*, with the vertical morphology of the latter remaining unknown as no resin/wax casting was attempted. More compacted mud patches host *Psilonichnus*-like crab-generated shafts (Fig. 7G). Other parts of the middle tidal flat are represented by a sandy flat densely

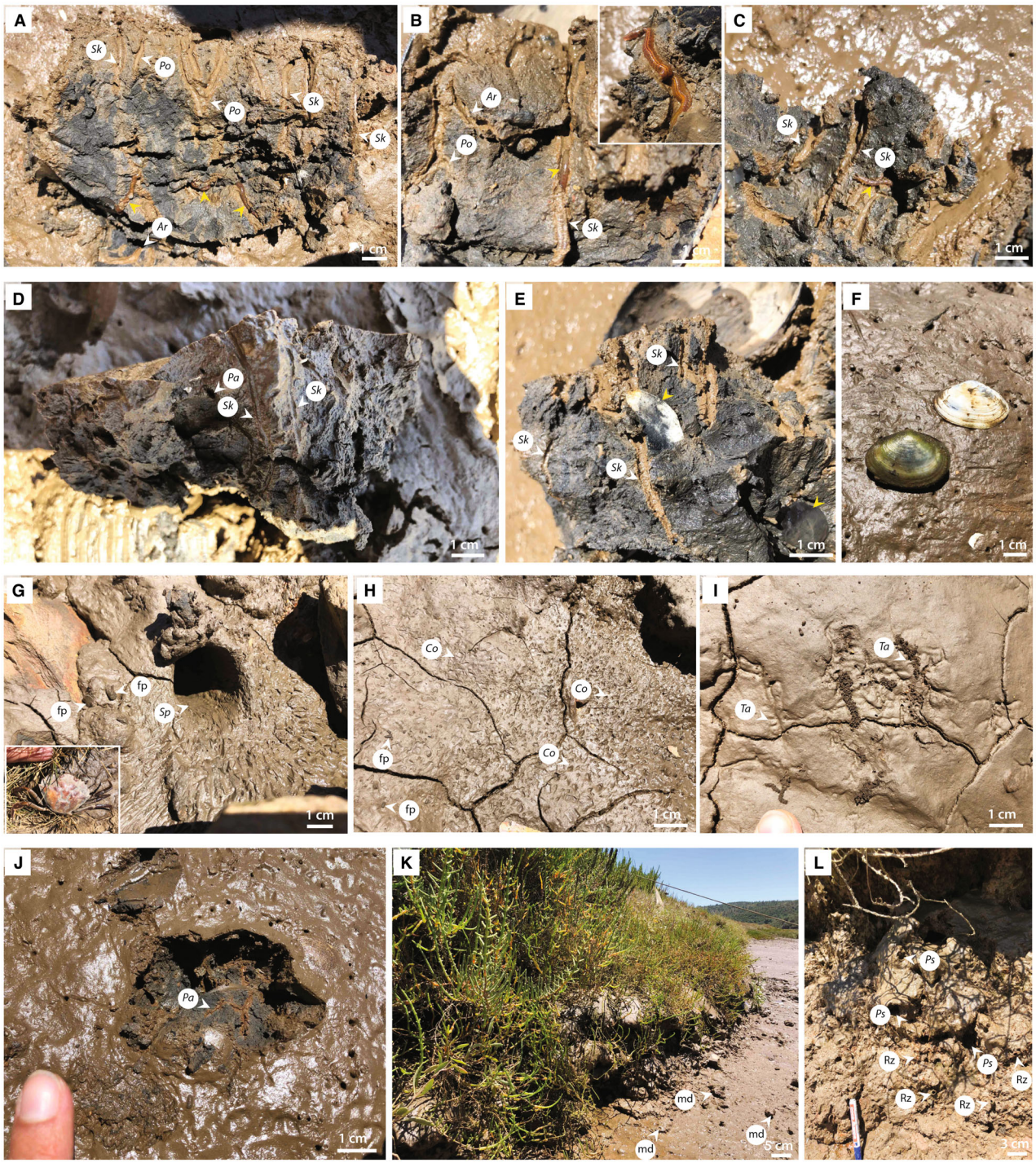

Fig. 6. Common trace-making organisms in the middle estuary (CBr) tidal flats and their burrows. (A, B) Polychaetes *Hediste diversicolor* (yellow arrows) in their burrows. *H. diversicolor* produces vertical, inclined, U- and Y-shaped, thickly lined burrows similar to *Skolithos* (*Sk*), *Arenicolites* (*Ar*) and *Polykladichnus* (*Po*). Inset: details of *H. diversicolor*. (C) Isopod *Cyathura carinata* (yellow arrow) produces thin, vertical to inclined burrows similar to lined *Skolithos* (*Sk*). (D) Thin and simple, vertical and horizontal burrows similar to *Skolithos* (*Sk*) and *Palaeophycus* (*Pa*). (E) Living shells and imprints of *Scrobicularia plana* (yellow arrows) in dysoxic black sediments forming simple, lined *Skolithos* (*Sk*) traces. (F) Disarticulated shells of *Scrobicularia plana* and *Spisula solida* on the tidal flat surface. (G) *Spongeliomorpha* (*Sp*) burrow entrances/exits with chelae marks and faecal pellets (fp). Inset: a carapace of *Carcinus maenas*. (H) Digit-like tracks and trackways (locomotion) similar to *Coenobichnus* (*Co*) and faecal pellets (fp) left by *Carcinus maenas/Uca tangeri*. (I) Back-filled excavations with small mud pellets attributable to *Taenidium* (*Ta*), likely formed by an insect or insect larvae. (J) Horizontal traces with Fe halo similar to *Palaeophycus* (*Pa*). (K) Upper tidal flat and marsh cliff covered in the growth of *Sarcocornia* sp. and *Artiplex* (*Halimione*) *portulacoides*. Mud clasts (md) are sourced from the marsh. (L) *Psilonichnus* burrows (*Ps*) made by *Uca tangeri*/*Carcinus maenas* with associated root penetration structures (Rz).

covered by *Zostera noltii* (rhizoliths; Fig. 7G, H), which becomes sparse towards the lower tidal flat. Rare patches of bare mud are colonized by bristle worms, *Capitella capitata* and *Hediste diversicolor* (Fig. 7I inset). These form traces similar to *Planolites, Palaeophycus, Skolithos, Arenicolites* and *Polykladichnus* (Fig. 7I). The substrate is colonized by deeply burrowing bivalves (e.g. *Scrobicularia plana*) found in a life position at a depth of ~40 cm and the common cockle *Cerastoderma edule* found disarticulated on the sediment surface. Both bivalves likely create vertical *Skolithos*, equilibrichnia-like 'siphonichnidal burrows' (e.g. *Siphonichnus, Scalichnus*), and cubichnia-like *Lockeia* with their siphon and foot.

The upper tidal flat is composed of 0.5 to 1 cm thick brownish muddy sand, underlain by ~1 cm of black, dysoxic mud (Fig. 7J, K) and a mixture of compacted sand and gravel beneath (Fig. 7L). It is covered in small burrow openings (1 to 2 mm in diameter), some of which appear dome-shaped on the surface due to coiled-up faecal strings. The burrows are vertical to subvertical, slightly curving and extend to a depth of 5 to 6 cm. They are likely produced by *Eisenia fetida* and *Arenicola marina* (Fig. 7J inset) and are similar to *Skolithos, Arenicolites* and *Diplocraterion* (Fig. 7J). U-shaped *Arenicolites* and *Diplocraterion* and Y-shaped *Polykladichnus* (Fig. 7K) are produced by *Corophium orientale, Cyathura carinata* and possibly by the polychaete *Pectinaria* (*Lagis*) *koreni*. Small gastropods with fusiform shells (2 to 3 mm in size) crawl on the sandy tidal flats, leaving *Archaeonassa*- and *Taphrhelminthopsis*-like traces. Vertical to inclined open shafts (~2 cm in diameter) similar to *Psilonichnus* are formed by variably sized *Uca tangeri/Carcinus maenas*. Several articulated and disarticulated shells of *Cerastoderma edule, Spisula solida* and *Ensis siliqua* (Fig. 7L inset) were also noted on the upper tidal flat, which may have produced *Skolithos* and 'siphonichnidal burrows' (Wetzel *et al.*, 2017; Wetzel & Unverricht, 2020), including *Siphonichnus* and *Scalichnus* (Stanistreet *et al.*, 1980; Zonneveld & Gingras, 2013; Knaust, 2015; Shchepetkina *et al.*, 2023) with their siphon and foot. Even though a shell of *Cerastoderma edule* was found in life position, no associated traces were noted. *Hediste diversicolor* is another important trace maker, creating mucus- and mud-lined, horizontal, vertical, inclined and Y-shaped traces similar to *Palaeophycus, Skolithos, Arenicolites*, *Diplocraterion* and *Polykladichnus*. Larger, horizontal burrows (5 to 10 mm in diameter) similar to *Planolites* and *Palaeophycus* (Fig. 7L) are likely the work of larger polychaetes and annelids such as observed *Hediste diversicolor* or previously recorded *Nepthys caeca, Boccardiella redeki* and *Alkmaria romijni* (Costa *et al.*, 2001). As for medium-sized (5 to 7 mm in diameter) *Planolites* and *Palaeophycus*, they are likely produced by *Eisenia fetida* and/or *Arenicola marina*. Even smaller (0.5 to 1 mm in diameter) vertical (-*Skolithos*-like) and horizontal (*Planolites*- and *Palaeophycus*-like) traces were observed to be formed by hair-like, red worms (*Capitella capitata* or *Heteromastus filiformis*). *Arenicolites*-like flexible tubes (>5 cm long) with an oxic halo, preferential grain selection and a whitish parchment-like material as a lining (Fig. 6J) are probably produced by *Arenicola marina* or *Chaetopterus varipedatus*.

Wherever the marsh zone exists, it presents *Psilonichnus*- and *Spongeliomorpha*-like burrows generated by *Uca tangeri*/*Carcinus maenas*, whereas vegetated cliffs are full of roots and root moulds.

Burrow distribution: Digital image analysis

Digital analysis of photographs collected in the field allowed the calculation of quantitative neoichnological parameters, such as open hole burrow density using a maxima mask in ImageJ, total burrow area, and minimum and maximum burrow diameter, to characterize the observed trace assemblage (Table 2, in grey). At the

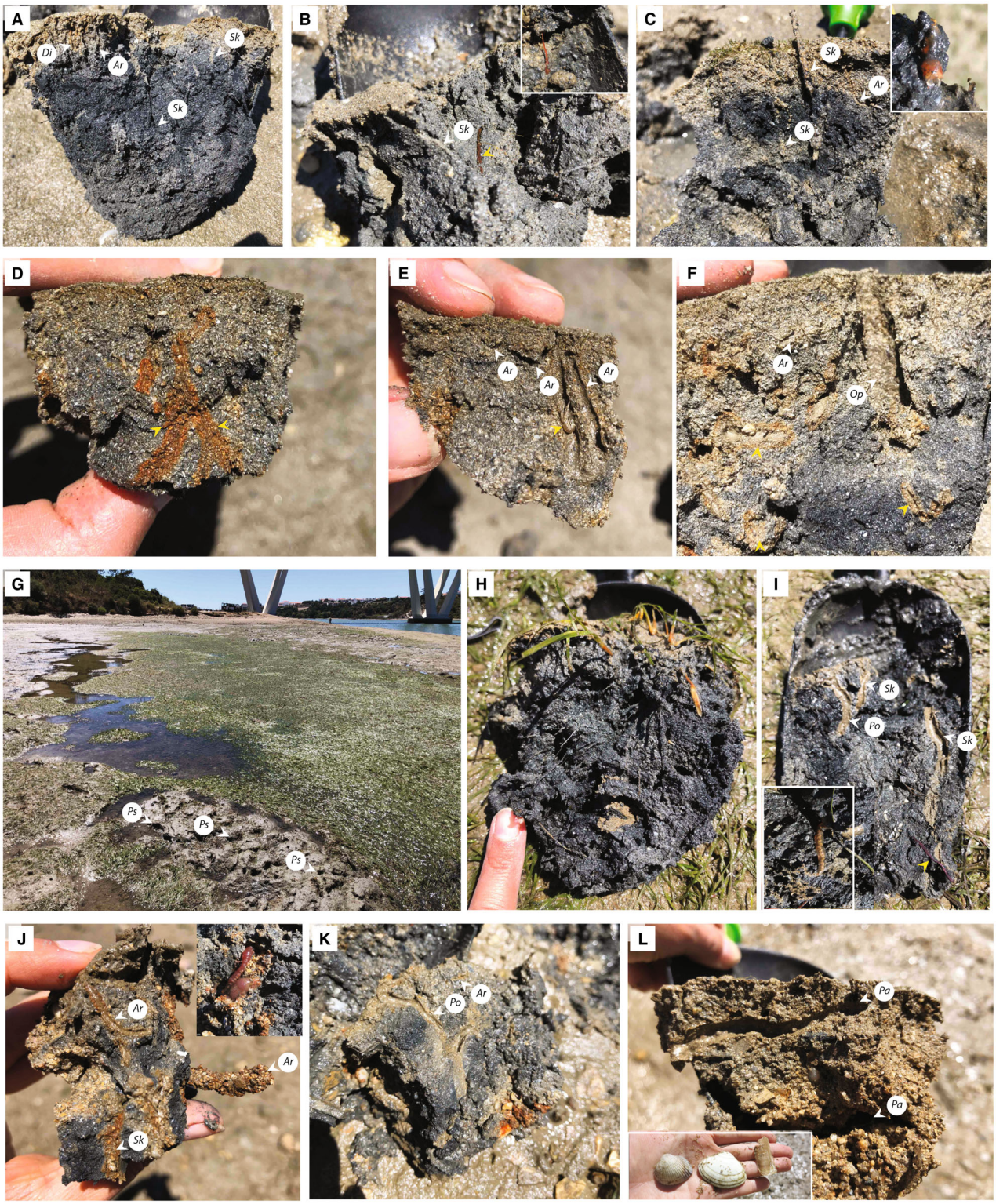

Fig. 7. Common trace-making organisms in the lower estuary (VNMF) tidal flats and their burrows. (A-B) Light-coloured oxygenated versus black dysoxic sand penetrated by thin vertical, inclined and U-shaped burrows attributable to lined *Skolithos* (*Sk*), *Arenicolites* (*Ar*) and *Diplocraterion* (*Di*) made by juvenile *Hediste diversicolor* (yellow arrow) and the hairworm *Capitella capitata* (see inset). (C) Thinly lined *Skolithos* (*Sk*) and *Arenicolites* (*Ar*) with whitish parchment-like material probably produced by *Arenicola marina* or *Chaetopterus varipedatus*. Inset: tube-living worm *Lagis koreni*. (D) Fe halos (yellow arrows) surround burrows located deeper in the substrate. (E) Smaller and larger *Arenicolites* (*Ar*) of *Corophium orientale* (yellow arrow) occupy the shallow tier. (F) *Arenicolites* (*Ar*) and knobbly *Ophiomorpha* (*Op*) in the lower tidal flat. Fe halos (yellow arrows) surround some deeper burrows. (G) Tidal creek and sandy tidal flat are covered by microscopic algae, *Spartina maritima*, and *Zostera noltii*. Eroded patches of firmer mud contain crab-produced traces similar to *Psilonichnus* (*Ps*). (H) A thin veneer of light-coloured, oxic sand on top of the dysoxic, black sand that is densely penetrated by roots of *Zostera noltii*. (I) *Skolithos* (*Sk*) and *Polykladichnus* (*Po*) burrows formed by *Hediste diversicolor* (inset) in tidal creek sediments. (J) *Skolithos* (*Sk*) and *Arenicolites* (*Ar*) flexible tubes with preferential grain selection and a whitish parchment-like material likely produced by *Arenicola marina* (inset) or *Chaetopterus varipedatus*. (K) *Polykladichnus* (*Po*) and *Arenicolites* (*Ar*) traces likely produced by *Corophium orientale, Cyathura carinata* and/or *Pectinaria* (*Lagis*) *koreni* in more cohesive substrates of the upper tidal flat. (L) Traces attributable to *Palaeophycus* (*Pa*) are likely produced by larger polychaetes and annelids. Inset: disarticulated shells *Cerastoderma edule, Spisula solida* and *Ensis siliqua* (left to right) found on the surface of the upper tidal flat.

middle estuary (CBr; Fig. 8A), the total area occupied by trace makers ranges from 0.8% to 4.1%, which equates to a bioturbation index of one to two (BI 1 to 2). Open burrow counts range anywhere from 4250 to 6700 burrows/m^2, while minimum and maximum burrow opening diameters (excluding open crab burrows) constitute 1.2 to 2 mm and 2 to 3.5 mm, respectively.

At the lower estuary (VNMF; Fig. 8B), the total burrow area equates to 1.4% and translates to a bioturbation index of one (BI 1). The burrow counts vary from 1550 to 3138 burrows/m^2, while minimum and maximum burrow opening diameters (excluding crab open burrows) constitute 2.1 to 2.6 mm and 3.6 to 4.7 mm, respectively.

CT scans

CT scans of push cores (35 to 50 cm long) provide a more complete picture of the bioturbation signature in the tidal sediments at both estuarine locations. The middle estuary tidal flats (CBr; Fig. 9) reveal heterogeneous and locally rhythmic substrates consisting of highly biogenically reworked (BI 4 to 6) intervals (often with biogenic mottling) and less bioturbated intervals (BI 1 to 3), showing better preservation of physical sedimentary structures (i.e. fine planar lamination, soft-sediment deformation, small-scale silt-loading and subtle current ripples). CT images also showcase a range of individual burrows such as *Arenicolites*, *Planolites*, *Lockeia*, *Scalichnus*, *Siphonichnus* and more rarely rhizoliths. Moreover, tiering relationships can be estimated. The shallow tier is predominantly represented by biogenic mottling, *Arenicolites*, and *Planolites*, with distributed gastropod debris and shell hash. The deeper tier is reflected by 'siphonichnidal burrows' similar to *Scalichnus* and *Siphonichnus, Arenicolites* and rarer rhizoliths.

The lower estuary tidal flats (VNMF; Fig. 10) also reveal interbedded sediments; however, these are of more variable lithology than those of the middle estuary. As well, these generally display lesser preservation and abundance of physical sedimentary structures, except for intervals with planar lamination (muddy) and massive bedding (sandy layers). Layering is only discernible due to the preservation of organic debris. In highly disturbed sediment layers, bioturbation intensity varies from BI 3 to 5, with the predominant bioturbation signature being cryptic or biogenically mottled. In less bioturbated sections, bioturbation intensity ranges from BI 1 to BI3. Individual burrows are visible on CT scans. When they are, in the shallow tier, they constitute burrows similar to *Skolithos, Arenicolites*, *Diplocraterion*, *Thalassinoides* and *Planolites*, whereas in the deep tier, 'siphonichnidal burrows', *Palaeophycus, Lockeia* and *Thalassinoides* are observed. The lower estuary cores also present elevated percentages of gastropods and shell hash.

DISCUSSION

Sediment distribution, organic matter and calcium carbonate content

The middle estuary location (CBr) is characterized by silty sand and sandy silt (Fig. 2A, Table 2), reflecting that moderate to low energy

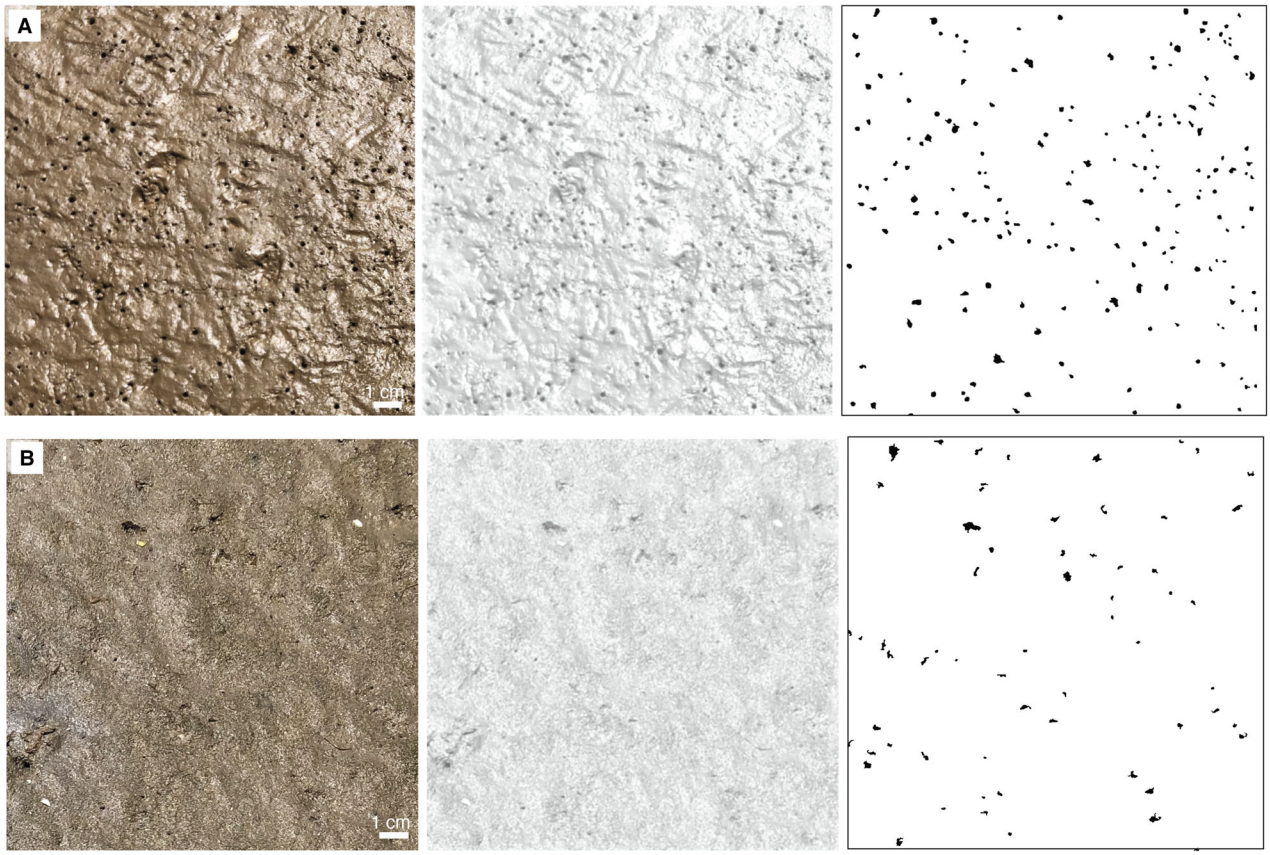

Fig. 8. An example of step-by-step ImageJ digital image analysis of the middle (A) and lower (B) estuary tidal flats, depicting the original photograph (left), its black-and-white version (middle) and finally a maxima mask (right). All images share the same scale as indicated on the original (left) photograph.

conditions prevail (Passega, 1964). Variations in the mean grain size indicate fluctuations in the hydraulic energy conditions during deposition, likely reflecting the interplay of fluvial and tidal currents. The sediments are also very poorly to poorly sorted, being symmetrical to predominantly fine skewed, and meso- to leptokurtic (Table 1).

The mean grain size of the lower estuary tidal flats (VNMF) is more variable (Fig. 2B, Table 2), ranging from very coarse silt to coarse-grained sand, recording deposition of coarser sediments (e.g. silty to gravelly sand). The sediments are predominantly very poorly sorted, very fine to fine skewed and show a wide range of graphic kurtosis (e.g. platykurtic to very leptokurtic; Table 1). These substantial changes in the statistical parameters point to higher variability in hydraulic energy and variable sediment sources at this location (e.g. fluvial, marine and local outcrops). Discrete lamina sets with positive and more rarely negative skewness likely indicate the bidirectionality of acting currents, recording flood and ebb tidal currents. Normally, the constancy of statistical parameters is attributed to the stability of hydraulic conditions within the environment (Martins, 1965). Herein, within both observed localities, the statistical parameters change, even though not dramatically, which can be interpreted as variability of hydraulic conditions within the estuary and seasonality of deposition.

As for the organic and calcium carbonate content (Table 2), on average, the organic matter content of the middle estuary tidal flats (CBr; 7.2%) is higher than that of the lower estuary (VNMF; 5.3%). This can be explained by the proximity to more extensive marsh areas in the middle estuarine reaches, as well as by the enhanced preservation potential of organic matter in finer, middle estuary sediments explained by suspension settling in association with

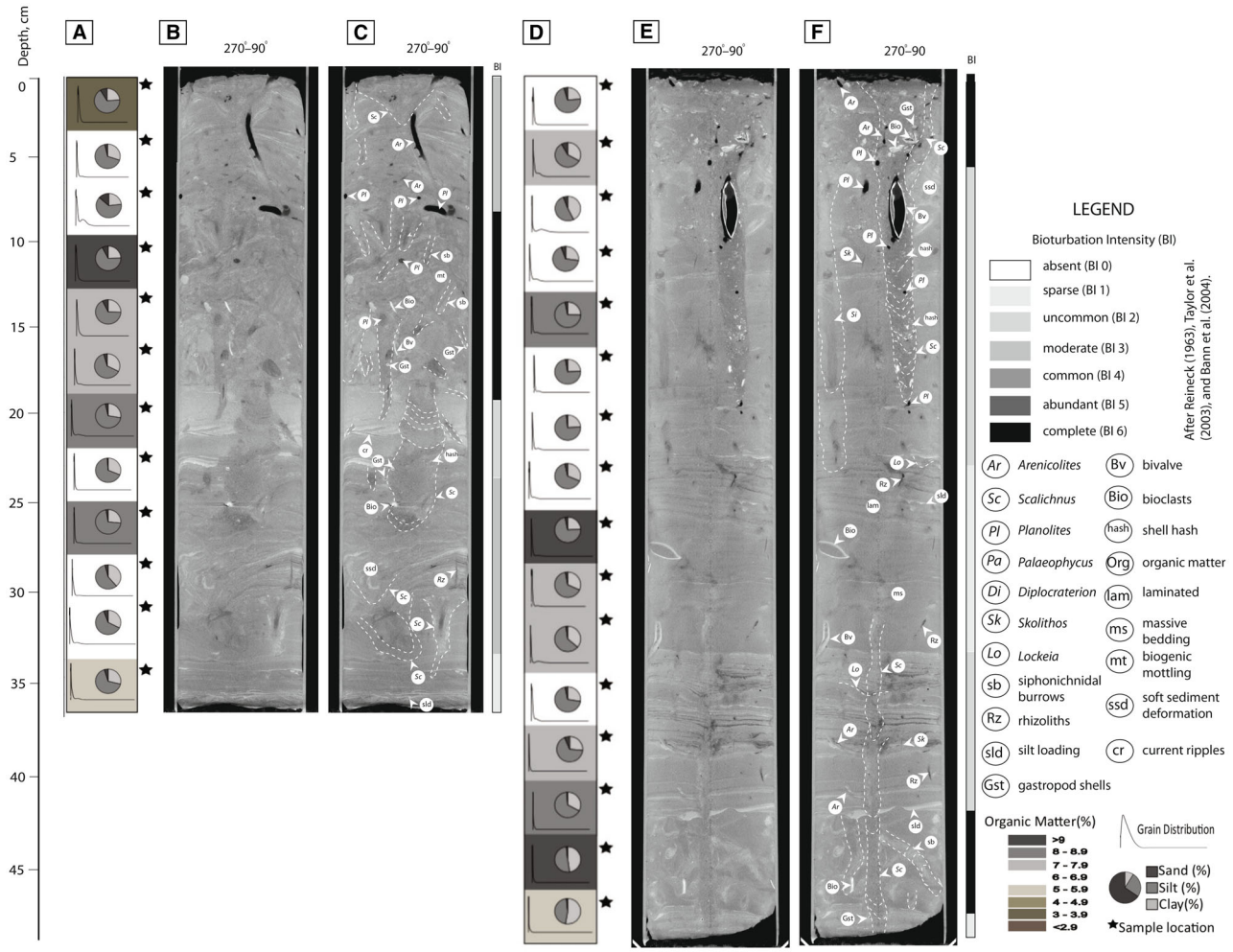

Fig. 9. High-resolution CT scans of two push cores from the middle estuary (CBr) tidal flat (for locations, refer to Fig. 1B) sliced at 270° to 90°. (A–C) Core CBR1T.F. (D–F) Core CBR2T.F. From left to right: core depth in cm; distribution of organic matter content (%) and grain size (sampled vertically along core every 3 cm); daylight photograph; annotated daylight photograph; and bioturbation index (BI). White dashed lines on (C) and (F) trace the morphology of more complex burrows such as *Siphonichnus* (*Si*) and *Scalichnus* (*Sc*).

fine-grained sediments (Yeo & Risk, 1981). Higher organic matter content translates to more organic matter available to intertidal macro- and microfauna, thus potentially explaining increased burrow counts from the middle in comparison with the lower estuary tidal flat surfaces (4250 to 6700 versus 1550 to 3138 burrows/m^2). Moreover, higher burrow counts may also be influenced by other factors, such as sediment grain size and the magnitude of salinity fluctuations. In contrast, the average calcium carbonate content of the middle tidal flats (1.6%) is much lower than that of the lower estuarine tidal flats (20.8%), indicating shell debris transported from the marine realm, higher growth rates of marine organisms with calcium carbonate shells and their broader availability downstream.

Grain size and statistical analyses of the vertical push cores introduce a temporal dimension to sediment distribution. The properties and characteristics of each core reflect the specific environmental conditions at their respective locations. The push cores recovered from the middle estuary location (CBr) exhibit a consistent composition. However, there are notable distinctions when compared to the push cores from the lower estuary (VNMF). The CBr cores are characterized by finer-grained sediment, primarily consisting of mud. Their deposition is a result of sediment sources (e.g. marshes, tidal flats and turbidity maxima) and

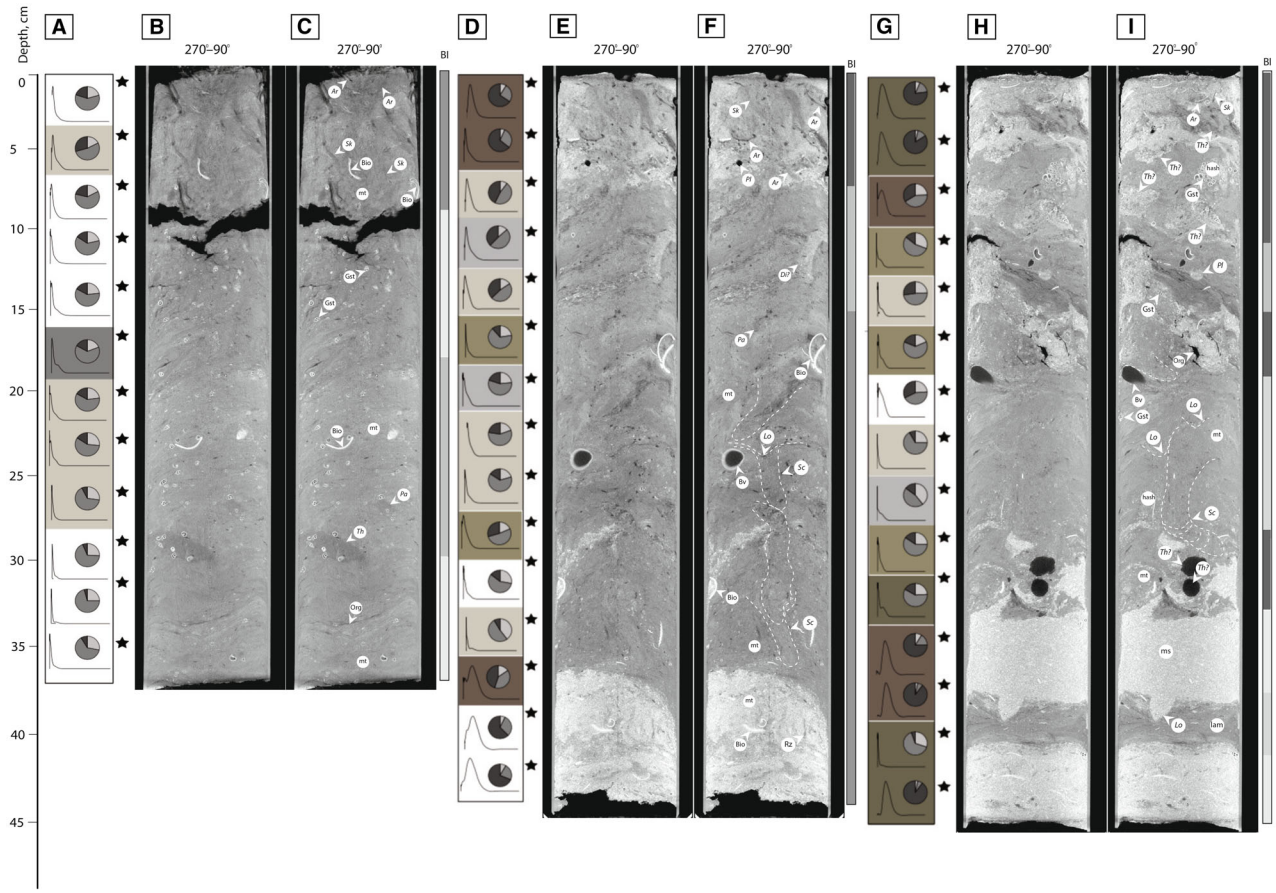

Fig. 10. CT scans of three push cores from the lower estuary (VNMF) tidal flat (for locations, refer to Fig. 1C) sliced at 270° to 90°. (A–C) Core VNMF 1; (D–F) Core VNMF 2; and (G–I) Core VNMF 3. From left to right: core depth in cm; distribution of organic matter content (%) and grain size (sampled vertically along core every 3 cm); daylight photograph; annotated daylight photograph; and bioturbation index (BI). White dashed lines trace the morphology of more complex burrows. Legend is the same as in Fig. 9.

the hydrodynamic activity (e.g. reworking, suspension) within the middle estuarine environment. The elevated organic matter content in these cores can be attributed to input from the surrounding salt marsh vegetation through time. Conversely, the carbonate content is low, indicative of scarce shell-bearing organisms within the sediments and/or faster dissolution of calcareous shells in the presence of elevated organic matter levels (Aller, 1994). A few coarse layers (sandy mud) may correspond to periods of heightened precipitation and subsequent increased fluvial discharge (i.e. river floods). Less likely, these layers could result from storm surges or more powerful spring flood tides (Yeo & Risk, 1981).

The VNMF cores are coarser, represented by sandy mud with several sandy layers, which are likely associated with hydrodynamic episodes characterized by increased energy dynamics (e.g. storm surges, stronger tidal currents). These cores show lower organic matter contents and heightened calcium carbonate contents, a scenario that can be explained by their increased proximity to the oceanic environment as described above. The distinct locations of the VNMF push cores, with VNMF1 being more distant from the main river channel and VNMF2 and VNMF3 being the closest, could contribute to the observed differences among them, expressed in varying bedding styles, sediment composition and trace assemblages. This is also evident in the gradient of calcium carbonate content, increasing from the middle to the lower tidal flat, from VNMF1 to VNMF2 and VNMF3.

Physico-chemical stresses

Physico-chemical stresses measured in the middle and lower estuary reaches impact the neoichnological character of the Mira tidal flats (Fig. 11). These include sediment grain size, substrate consistency, subaerial exposure, water salinity, pH, temperature and oxygenation. The grain size of the substrate is controlled by the Mira River transport capacity and the lithological characteristics of the source rocks, whereas substrate consistency depends on the length of subaerial exposure, which in turn is determined by tidal flat elevation (i.e. its terrace levels). High marsh and upper tidal flat sediments of the CBr middle estuary tend to be finer-grained and more compacted, due to prolonged subaerial exposure. By contrast, the lower-middle tidal flats are characterized by siltier and sandier compositions overlain by fluid to semi-consolidated mud (up to 10 cm thick).

The VNMF lower estuary tidal flats contain coarser sediments in their upper part and slightly finer, better-sorted sediments towards the lower-middle tidal flat. Such an inverse relationship is due to the upper tidal flat being located near erosionally receding cliffs, which source gravel-sized sediments and contribute to the gravelly sand and gravelly muddy sand compositions. The sandy portion is likely locally transported from nearby sandy beaches by tidal or wave action, while riverine currents bring silt and clay in suspension. Similar to the CBr middle estuary, substrate consistency on the VNMF tidal flats changes according to the topographic position, with marshy areas containing more compacted sediments.

Lowered and/or fluctuating salinity has been considered one of the main stress factors affecting infauna in estuarine settings (Remane & Schlieper, 1971; Grassle & Grassle, 1974; MacEachern & Gingras, 2007; Gingras *et al.*, 2011). In the Mira system, the middle estuarine waters (CBr) have lower salinity levels that range from 24.7 to 28.9‰ compared to the lower estuary (VNMF), which shows salinities ranging from 35.0 to 35.3‰ (Table 2). This demonstrates a typical estuarine gradient, where salinity increases in the seaward direction (Fig. 11; Dörjes & Howard, 1975; Howard *et al.*, 1975; Brown *et al.*, 2002a; Adão *et al.*, 2009; Solórzano et al., 2017). Salinity in the Mira River estuary also increases with the incoming tide, when the salt wedge is pushed upstream, especially during spring tides (Table 2; Paula, 1998; Medeiros *et al.*, 2012; Fatela *et al.*, 2016). A more significant salinity increase was observed in the middle estuary at the CBr site from low to high slack-water periods, with a change of 4.2‰. By contrast, in the lower estuary at the VNMF site, salinities only increased by 0.3‰. This disparity is a consequence of a very low fluvial discharge in summer months and during dry periods (Fig. 12A) that leads to more stable marine influence in the lower estuary during both low and high tides.

The physico-chemical gradient along the Mira River estuary is corroborated by the historically averaged pH values that point to brackish water at the CBr middle estuary. At CBr, the estimated pH values are below normal pH for marine water (8.1 to 8.3; e.g. Brown *et al.*, 2002b), increasing from 7.7 to 8.0 with the rising tide and the consequent upstream migration of a salt wedge (Table 2). The pH values measured at the VNMF site at low (8.1) and high slack-water periods (8.2) confirm that the Mira lower estuary has no significant fluvial influence and remains permanently under marine influence, particularly during dry seasons (Fig. 12A).

The seasonal coastal upwelling that occurs along the western Iberian Peninsula from April to October (e.g. Fiúza, 1983; Relvas *et al.*, 2007, and references therein) is responsible for the temperature drop with the incoming tide in the Mira River estuary. In the middle (CBr) and lower (VNMF) estuary, the temperature decreases by 0.7°C and 4.8°C, respectively (Table 2). The more significant temperature drop in the lower estuary is a result of the larger (and colder) tidal prism near the estuary mouth, where it transitions into the open sea.

Dissolved oxygen concentration is another crucial parameter that can influence infaunal activity and lead to reductions in benthic animal populations (Dashtgard *et al.*, 2015). The rising tide has a complex effect on dissolved oxygen concentration, especially in the Mira River and Sado River estuaries (Matos, 2008). Most Portuguese rivers have a drainage direction to the W or SW, including rivers like Minho, Lima, Douro, Mondego and Tagus. However, both the Mira and Sado drain towards the N-NW due to tectonic constraints (i.e. faults, structures). Because the Mira River estuary lies within a plateau that forms a canyon and with the middle estuary location (CBr) aligned NNW–SSE (Fig. 1A), it is dominated by strong NE-N-NW winds

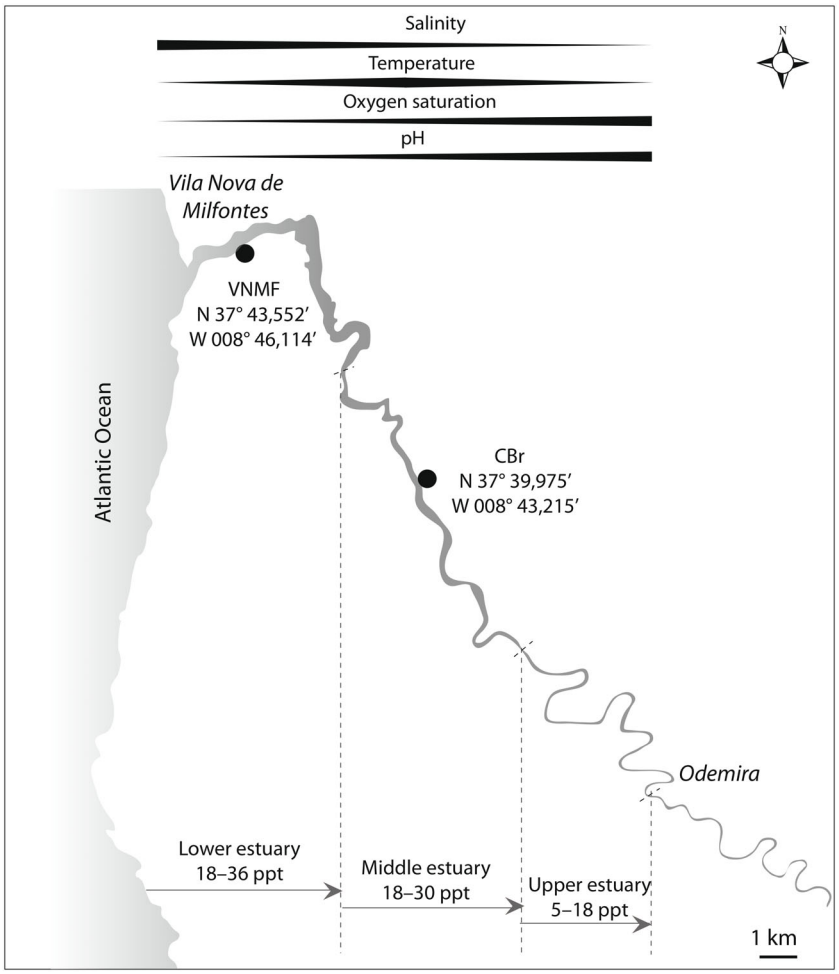

Fig. 11. Changes in measured physico-chemical parameters (i.e. salinity, temperature, oxygen saturation and pH) along the Mira River estuary with coordinates of the middle (CBr) and lower estuary (VNMF) study sites. Thicker black lines represent an increase in the measured parameter, while thinner black lines indicate a decrease.

blowing during summer (Fig. 12B). These winds funnel through the canyon and create small waves called fluvial wavelets. As the outgoing tide moves against the wind, it causes friction at the water–air interface. The wavelets increase surface agitation, enhancing oxygen exchange and improving water oxygenation (Downing & Truesdale, 1955; Moutzouris & Daniil, 1995; Ribaudo *et al.*, 2021). This leads to a varied response of dissolved oxygen levels between the lower and middle sections of the estuary. Thus, in the lower estuary (VNMF), dissolved oxygen increases from 63.5 to 63.9% with the rising tide, adding to the dynamic changes governed by the tides (Table 2). However, in the middle estuary (CBr), dissolved oxygen decreases from 89.4 to 75.7% with the rising tide (Table 2). This inverse relationship may be linked to the geomorphological peculiarity of the Mira River, where wavelets preferentially develop during falling tide in the middle estuary and increase its dissolved oxygen levels.

Trace makers

Vermiform invertebrates (e.g. polychaetes, nemertines, annelids and tube worms), amphipods, bivalves and crustaceans constitute most of the burrowing macrobenthos observed along the Mira River estuary. Similarly, Costa *et al.* (2001) reported that mudflats of the middle Mira River estuary are dominated by deposit feeders such as copepods, amphipods and polychaetes (e.g. *Hediste diversicolor, Nepthys caeca*), whereas the lower parts of the estuary

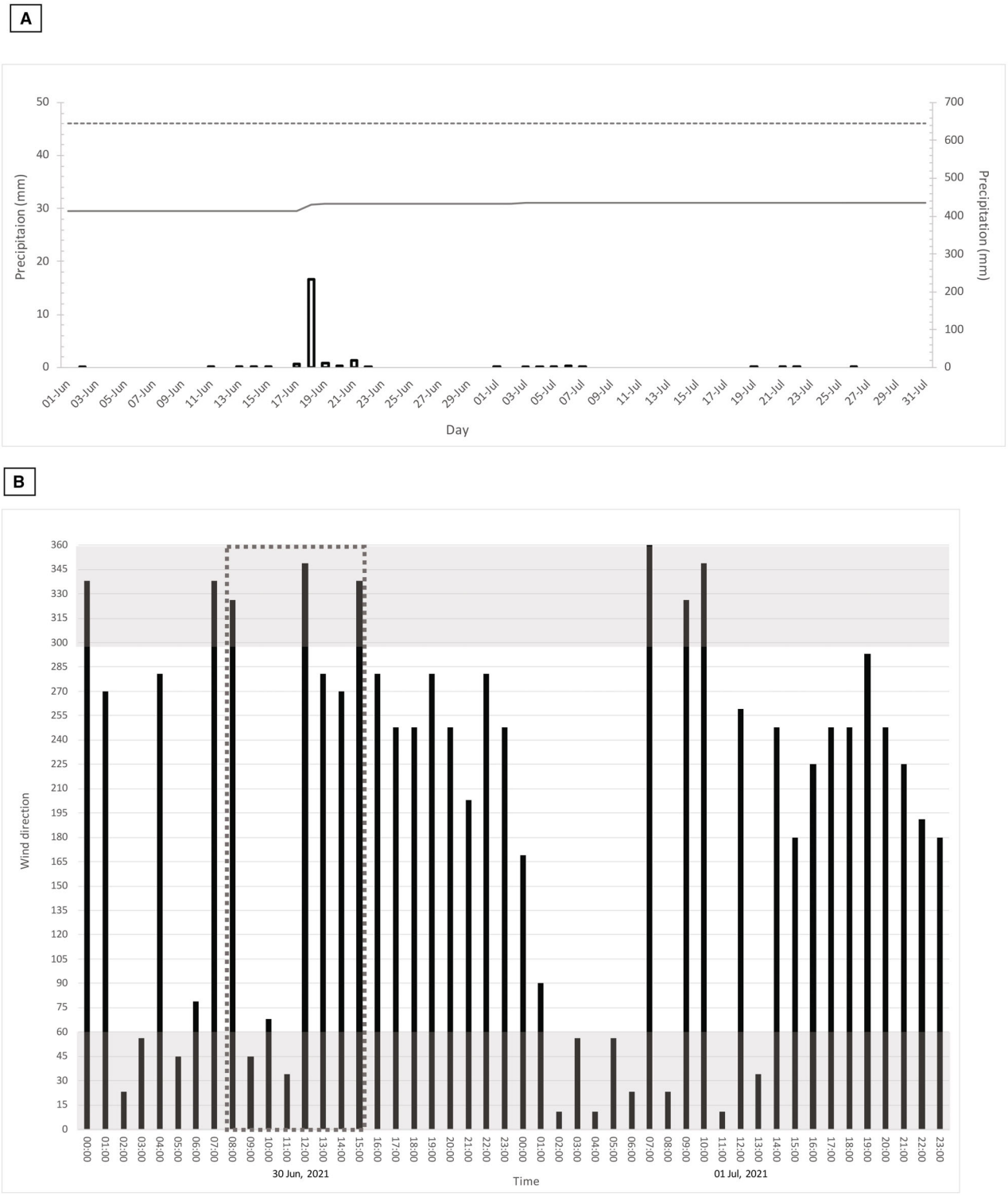

Fig. 12. (A) Precipitation records in the Mira River basin. Left scale: daily precipitation values from 1 June to 31 July 2021. Right scale: cumulative precipitation from 1 June to 31 July 2021 (black solid line) and mean annual precipitation for 30 years (dashed grey line). (B) Wind direction hourly records in the Mira River basin from 30 June to 1 July 2021. Lower grey rectangle: N-NE sector. Upper grey rectangle: N-NW sector. Dashed rectangle: Wind dominant direction during tide out (NW-N-NE), before the CBr water parameters were measured. Source: Serviço Nacional de Recursos Hídrico—Agência Portuguesa do Ambiente, http://snirh.apambiente.pt (02.08.2023).

are inhabited by bivalves, such as the peppery furrow shell *Scrobicularia plana*, which use siphons for surface feeding by extracting detritus from the tidal flat sediments and for suspension feeding by filtering particles from the water column. Other detritus feeders observed in the present study, such as *Carcinus maenas* and *Uca tangeri*, are widespread both in the middle and lower estuarine reaches, whereas other crustaceans (i.e. shrimps) use salt marsh and mud tidal flats to feed on polychaetes, meiofauna and detrital material. The burrows produced by vermiform organisms, isopods, amphipods and crustaceans tend to represent dwelling and feeding structures similar to *Skolithos, Arenicolites, Diplocraterion, Polykladichnus, Ophiomorpha, Planolites*, *Palaeophycus* and *Thalassinoides*. Although the burrow orientation of *Polykladichnus, Arenicolites, Palaeophycus, Thalassinoides* and *Skolithos* may appear similar or intergradational in cross-sections (Dashtgard, 2011a), potentially produced by the same burrower in this estuarine study, this is not universally the case. These burrows tend to have a very simple morphology (e.g. vertical, inclined and U-shaped), rarely branch, are smooth-walled and are nearly always mucous lined. They are predominantly observed within the shallow tier in both fine- and coarser-grained sediments of the middle and lower estuary and occur in intervals characterized by high bioturbation intensity (BI 4 to 6) and lower organic matter content. Thus, decreased organic matter can be attributable not only to coarser grain size but also to higher degrees of bioturbation and infauna actively processing food resources found *in situ* in intertidal flats (Dashtgard, 2011a).

In the Mira River estuary, 'siphonichnidal burrows' (i.e. *Scalichnus, Siphonichnus*), *Lockeia*, fugichnia and *Skolithos* are commonly associated with filter-feeding bivalves (e.g. *Scrobicularia plana, Corbicula fluminea* and *Cerastoderma edule*), where the burrow structure is variable based on bivalve functions. 'Siphonichnidal burrows' likely reflect the activity of bivalve siphons, and most bivalves use siphons for filter feeding, thus representing domichnia and equilibrichnia. *Lockeia* indicates cubichnia, whereas *Skolithos* evidences permanent dwelling (domichnia) and, less so, bivalve filter-feeding activity with siphons. Bivalves are also capable of moving short distances both vertically and horizontally within the sediment, creating vertically stacked burrows (Figs 9 and 10) interpreted as equilibrichnia and fugichnia with some lateral migration (Fig. 9). These bivalve-generated structures are predominantly preserved in the deeper tier due to bivalve infaunal lifestyle preferences, keeping them out of reach of erosional processes and predation (Wetzel & Unverricht, 2020). A detailed description of bivalve-generated trace morphology and taphonomy in the Mira River estuary was previously outlined in Shchepetkina *et al.* (2023).

The last major group of burrowing infauna constitutes the crustaceans, especially the shore crab *Carcinus maenas* and fiddler crab *Uca tangeri*. These crabs leave a variety of traces (e.g. *Psilonichnus, Spongeliomorpha, Coenobichnus*, scratch marks (?), faecal pellets similar to *Favreina* Brönnimann, 1955) (in Knaust, 2020). These traces represent different burrowing crab behaviours such as dwellings, crab locomotion, surficial feeding, excretion and biodeposition, reflecting such biotic parameters as the age of the trace maker and such physico-chemical processes as tidal cycles (i.e. high/low tide), salinity, time of the day, substrate moisture and marsh root density (Shchepetkina, 2025).

A potentially overlooked group of trace makers in the Mira is represented by subtidal feeders (e.g. Sparidae fish). Muñiz *et al.* (2015) and Belaústegui & Muñiz (2016) reported from the Piedras River (Lepe, Huelva, SW Spain) that Sparidae fish are capable of leaving bite marks, producing 'cruzianaeform' traces when grazing and feeding on the bottom of tidal flats. Even though these fish were not observed during fieldwork by the authors, the crab-generated scratch marks reported in Shchepetkina (2025) might represent fish bilobed bite traces. This observation is in line with the one made by Gingras *et al.* (1999) in Willapa Bay, where they recorded feeding pits left by *Dungeness* and sturgeon when venturing onto tidal flats in search of food.

Cryptobioturbation, indicated by extensive biogenic mottling observed in CT scans of push cores, reflects the activity of meiobenthos. Moreover, surface tracks and scratch marks as visible in Figs 4C, 6H, and 8 would also contribute to biogenic mottling in the mixed layer or upper tier. While semi-quantification of cryptobioturbation was not undertaken in this study, burrows of small polychaetes (e.g. threadworms) were observed in shallow trenches, and nematodes and copepods have been previously documented in the Mira tidal flats (Adão *et al.*, 2009; Alves *et al.*, 2009). Cryptobioturbation and biogenic mottling appear localized in the middle

estuary push cores and more abundant in the lower estuary push cores; however, it cannot be reliably distinguished from successive tiering or overprinting of biogenic structures.

Neoichnological distributions and controls on bioturbation

Both plan view observations of tidal flats and CT imaging of push cores indicate that the diversity of traces and intensity of bioturbation across the Mira tidal flats is heterogeneous, changing vertically as well as across the tidal flats (Fig. 13). For example, low-middle intertidal zones of the middle estuary (CBr; Fig. 13A) are characterized by moderately to highly diverse, vertical to inclined, simple, thickly lined and shallowly penetrating burrows such as *Skolithos, Arenicolites, Diplocraterion, Polykladichnus*, *Palaeophycus* (except for deeper penetrating 'siphonichnidal burrows') and surficial scratch marks/'cruzianaeform', which change laterally to an assemblage of *Arenicolites, Diplocraterion*, *Palaeophycus*, scratch marks/'cruzianaeform', faecal pellets and deeper penetrating *Thalassinoides* and 'siphonichnidal burrows' towards the middle-upper intertidal flat. These give way, finally, to a less diverse, more continental assemblage of traces similar to *Taenidium, Planolites, Coenobichnus*, *Psilonichnus, Spongeliomorpha*, faecal pellets and root traces in the marsh area (Fig. 13A). As such, from an ichnological perspective, tidal flat sediments in a tide-influenced, mud-dominated middle estuary would be represented in the rock record by a predictable progression of trace fossils. In the lower to middle intertidal zone, the sediments would contain mostly shallow dwelling structures produced by siphon-feeding organisms, with occasional deposit-feeding traces. These would transition in the middle to upper intertidal zone into a combination of surface locomotion traces and deeper-tier deposit-feeding and siphon-feeding structures. Finally, the high intertidal to supratidal zone would be characterized by sediments containing permanent vertical to inclined dwellings, continental biogenic structures and surface locomotion traces (Fig. 13). Digital analysis using ImageJ reveals minimal variation in the size of open-hole burrows across the three middle estuary sites, with diameters ranging from 1.2 mm to 3.5 mm, excluding larger burrows created by crabs. As for the intensity of bioturbation, bedding-plane bioturbation intensity barely changes (BI 0 to 2; Fig. 8A), while vertically, BI changes significantly from BI 1 to 3 to 4 to 6 (Fig. 9).

In the lower estuary (VNMF; Fig. 13B), similar changes in the neoichnology are observed. Moderately diverse and shallow-penetrating traces similar to *Skolithos, Arenicolites, Diplocraterion* (some with parchment-like linings), *Polykladichnus*, *Palaeophycus, Lockeia*, rhizoliths and slightly deeper penetrating *Ophiomorpha, Thalassinoides* and 'siphonichnidal burrows' characterize the lower-middle sandy tidal flats, which change laterally to an assemblage dominated by low-moderate diversity of *Polykladichnus, Skolithos, Arenicolites, Palaeophycus* and rare *Thalassinoides* in the upper intertidal zone. This gives way to a low-diversity, more continental assemblage dominated by root traces, *Psilonichnus* and *Spongeliomorpha* near the marsh area. From a paleoichnological standpoint, tidal flat sediments of a tide-influenced, mud-dominated lower estuary would be reflected in the rock record as a succession of ichnoassemblages reflecting environmental gradients. The lower intertidal zone would be characterized by shallow to somewhat deeper, dwelling structures of suspension and siphon feeders, rarer deposit feeders, resting traces and rhizoliths, transitioning into slightly deeper, dwelling burrows of suspension and, more rarely, deposit feeders in the middle tidal flat. This would be capped by a continental assemblage of crab dwelling burrows interspersed with rhizoliths (Fig. 13). Digital analysis using ImageJ shows that open-hole burrows in the lower Mira estuary are larger than those observed in the middle estuary, with diameters ranging from 2.1 mm to 4.7 mm, excluding larger crab-generated burrows, likely explained by higher salinity levels and slightly lower water temperatures (e.g. Buatois *et al.*, 2005; Gingras *et al.*, 2007, 2011). Surficial BI remains relatively consistent across the lower estuary tidal flats (BI 0 to 1; Fig. 8B). In contrast, vertical BI exhibits greater variability, ranging from BI 1 to 3 to BI 3 to 5 (Fig. 10).

Both recorded neoichnological trends (CBr and VNMF) reflect various *environmental gradients* across the tidal flats and are the result of organism behaviours principally controlled by substrate consistency, duration of subaerial exposure, sediment grain size (e.g. sandy tidal flats versus muddy tidal flats), rates of sediment deposition and biogenic reworking, salinity, energy conditions at the bed, types of food and its availability, oxygenation, temperature

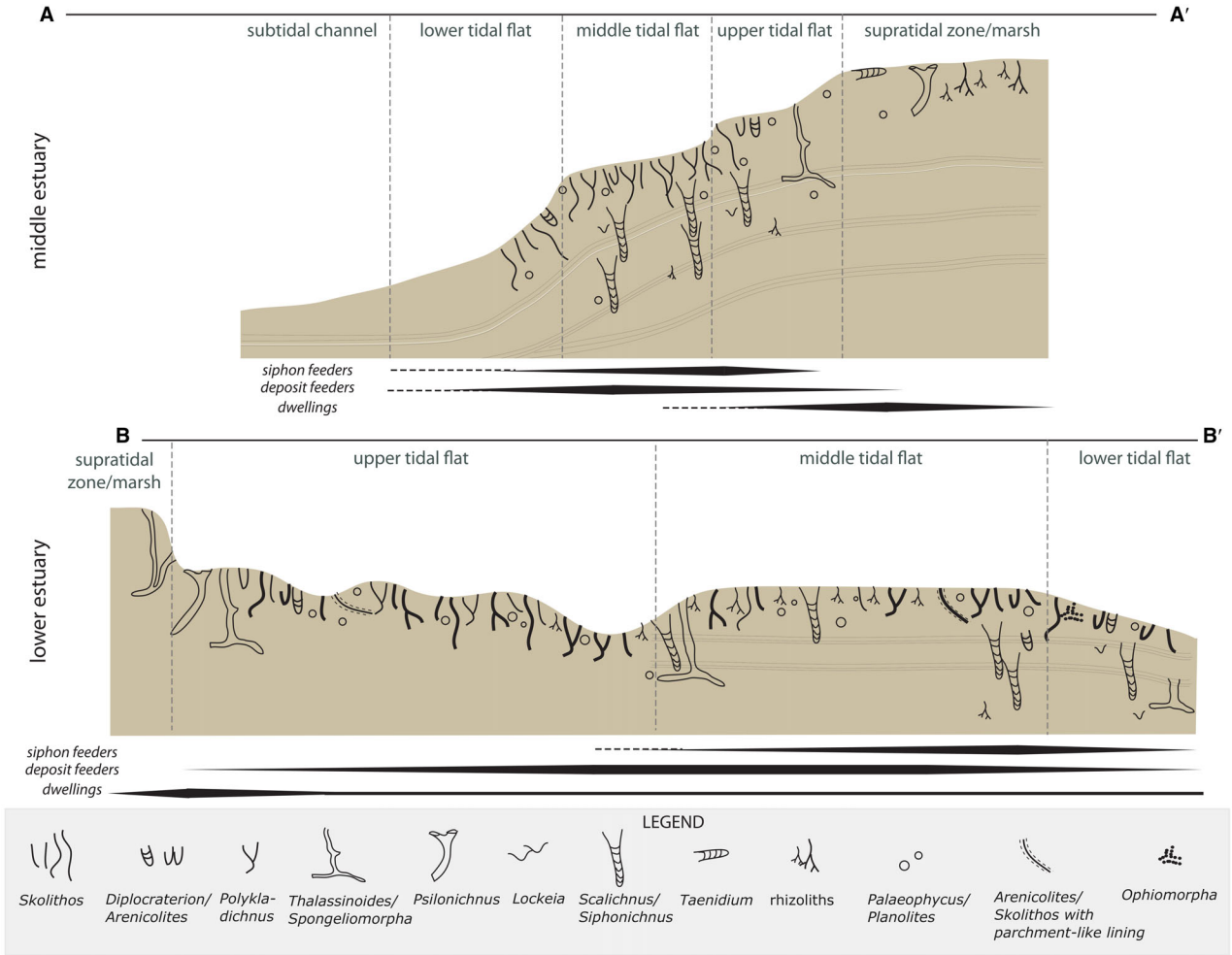

Fig. 13. Schematic diagrams of ichnological assemblages at the middle (A) and lower (B) estuary tidal flats along A to A′ and B to B′ lines (for cross-section position, refer to Fig. 2). Thickness of the lines/burrows indicates size of their producers, with the lower estuary characterized by increased trace size.

and pH (Howard, 1975; Frey, 1978; Savrda *et al.*, 1984; Gingras *et al.*, 1999; MacEachern *et al.*, 2012).

Sediment texture, grain size and *consistency* are some of the most important factors controlling the trace distribution on the middle and lower estuary tidal flats. For example, in the middle estuary tidal flat (CBr), where up to three terraces are present (corresponding to the lower, middle and upper tidal flat) (Figs 2, 4A and 13), sediment texture and consistency vary. The upper 3 to 10 cm of substrate on the lower and middle terraces consists of unconsolidated sediments with a soft to locally fluid consistency. Such consistency is often referred to as a 'soupground' (Ekdale, 1985; Gingras *et al.*, 2000) and shows minimal bioturbation, as infauna has to 'swim' through the sediments (Lobza & Schieber, 1999), resulting in indistinct traces known as 'biogenic mottling'. Slightly more consolidated sediments below 3 to 10 cm of depth and higher towards the middle and upper tidal flat consist of muddy softground fully covered in crab-generated scratch marks (Shchepetkina *et al.*, 2023), which might alternatively represent fish-generated 'cruzianaeform' fish bite marks (Muñiz *et al.*, 2015; Belaústegui & Muñiz, 2016), and open, well-maintained dwelling and sediment feeding structures often impregnated with mucus. This soft, muddy substrate is dominated by bivalves, polychaetes and burrowing crustaceans similar to other examples provided by Dashtgard *et al.* (2008) and Yang *et al.* (2009). The substrate found higher up is stiffground

(Lettley *et al.*, 2007), often with a mud-cracked surface. It is consolidated and de-watered enough for fauna to maintain wide, open burrows without mucus and linings similar to *Spongeliomorpha* and *Psilonichnus* (Figs 4C and 13; Gingras *et al.*, 2000; Gingras & Bann, 2006; Lettley *et al.*, 2007; La Croix *et al.*, 2022).

It is not only sediment consistency but also the increased duration of *subaerial exposure*, being the function of elevation and tidal range that can explain the change in trace ethology across the tidal flats. With increased subaerial exposure (i.e. towards the supratidal zone and marsh), the diversity and population density of burrowing animals decline, with polychaetes and bivalves being replaced by crustaceans, which are better adapted to withstand physico-chemical stresses caused by prolonged subaerial exposure (Häntzschel, 1939; Swinbanks & Murray, 1981; Gingras *et al.*, 1999; Pearson & Gingras, 2006; Dashtgard, 2011a) and as a result of adaptations to a fossorial mode of life (Koo *et al.*, 2007).

The lower estuary (VNMF) is defined by higher sand content and less developed terracing, thus having a more uniform distribution of traces (Fig. 13). Sandy sediments, especially the fine- and medium-grained sands, are more prone to rapid reworking by infauna (Alexander *et al.*, 1993). Coarser sediment grain size also leads to more sediment instability, forcing trace makers to stabilize their burrows with mucus lining, sediment pellets (e.g. *Ophiomorpha*) or parchment-like linings (Bromley, 1996; Dashtgard *et al.*, 2008; Dashtgard & Gingras, 2012), as often observed in the Mira tidal flats.

Seasonal variations in rates of bioturbation and *sedimentation* are likely responsible for differences in the observed bioturbation intensity for both the middle and lower estuary. Although the low and stable plan-view bioturbation intensity (BI 0 to 2) does not fully equate to the vertical BI and should be higher, being based solely on vertical and subvertical burrow openings and excluding crab burrows and surface biogenic structures, it still likely reflects a short-term 'snapshot' of benthic conditions (Marenco & Bottjer, 2010). On the contrary, a drastic change in BI in a cross-sectional view (BI ranging from 0 to 6) indicates seasonality of deposition, where strongly burrowed intervals reflect lower sedimentation rates and higher rates of biogenic reworking (Gingras *et al.*, 1999; Gingras *et al.*, 2025). The observed discrepancy in BI between the plan and cross-sectional views is partially indicative of the cumulative effects of both physical and biological conditions that operate over longer time periods (Marenco & Bottjer, 2010), where the sediments are reworked by successive generations of infauna (Dashtgard, 2011a, 2011b; Ayranci *et al.*, 2014). It is also possible that plan- and cross-sectional views reflect different burrow morphologies and various orientations of the 2D view of burrows (McIlroy, 2004; Eltom *et al.*, 2022; Melnyk *et al.*, 2025). It is important to note, however, that most likely, the BI measured in plan view is limited and represents only a minimum estimate, as it is based solely on visible open vertical and subvertical burrow openings and excludes other burrow morphologies, orientations, and surface biogenic structures.

Salinity in the Mira River estuary has been identified as the primary stress factor affecting infaunal distributions (Medeiros *et al.*, 2012). The brackish-water conditions in estuaries change temporally on semi-diurnal and seasonal time scales (Chapman, 1981; Gingras *et al.*, 1999; La Croix *et al.*, 2015; La Croix & Dashtgard, 2015) and spatially along the estuary, creating the so-called physico-chemical gradient between the freshwater, brackish-water, and fully marine reaches (Fig. 11; Dörjes & Howard, 1975; Howard *et al.*, 1975; Alves *et al.*, 2009; Medeiros *et al.*, 2012). Temporal variations in trace distributions in the Mira are also often attributed to the seasonality of climate and variations in fluvial flux (Medeiros *et al.*, 2012; Fatela *et al.*, 2016), where variations in fluvial discharge or the amount of rain (Fig. 12A) may lead to seasonal shifts in the propagation of the salt wedge and turbidity maximum, thus affecting the nature of the substrate and infaunal colonization (Gingras *et al.*, 2002b; Buatois *et al.*, 2005). Temporal and spatial variations in meiofaunal distributions have also been well-documented (Heip *et al.*, 1985; Austen & Warwick, 1989; Moens & Vincx, 2000; Steyaert *et al.*, 2003). Salinity fluctuations and overall low salinity are well-known to place limitations on the size of burrowers by impairing their ability to regulate ionic and osmotic balance and disrupting the maintenance of cellular fluid chemistry (Croghan, 1976; Felder, 1978; Pequeux, 1995). The trend of trace size diminution up-estuary observed in the Mira is corroborated by other neoichnological studies (e.g. Heckel, 1972; Pemberton *et al.*, 1982; Gingras *et al.*, 1999, 2011, 2012; Gunn *et al.*, 2008; Hauck *et al.*, 2009; Shchepetkina *et al.*, 2016b).

Decreasing salinity has also been reported to lead to a decrease in the density and diversity of burrowing organisms landward. However, in the case of the Mira River estuary as well as the Fraser River delta (BC, Canada; Dashtgard *et al.*, 2008; Dashtgard, 2011a, 2011b), a decrease in salinity does not correspond to a decrease in trace diversity and a range of burrowing behaviours. In contrast, both increase towards the muddier middle estuary locale. Such a contradiction might signal that trace diversity is not only controlled by salinity but is also strongly influenced by substrate conditions, with finer-grain size being more favourable to infaunal colonization (Dashtgard *et al.*, 2008; Dashtgard, 2011a, 2011b; Ayranci *et al.*, 2014), by increased oxygenation, better *food availability* (higher organic matter %) and the adaptability of the benthic community to fluctuating and decreased salinity.

The Mira River estuary neoichnological trends are similar to other reported brackish water ichnocoenoses, being typified by (1) an overall low to moderate ichnodiversity (Figs 6, 7 and 13, Table 2), (2) relatively high trace density (Figs 8 to 10, Table 2) with the sediment surfaces being highly reworked overall, as well as in the push cores, (3) traces decreasing in size landward (Table 2) and (4) an infaunal assemblage of simple vertical and horizontal traces (e.g. Pemberton *et al.*, 1982; Beynon *et al.*, 1988; Pemberton & Wightman, 1992; Gingras *et al.*, 1999; Pearson & Gingras, 2006; Gingras *et al.*, 2011; Shchepetkina *et al.*, 2016b; Gingras *et al.*, 2025). Similar to other neoichnological studies conducted on the Fraser River delta (BC, Canada; Dashtgard *et al.*, 2008; Dashtgard, 2011a, 2011b), Willapa Bay (USA; Remane & Schlieper, 1971; Clifton & Phillips, 1980; Gingras *et al.*, 1999), Kouchibouguac Bay (NS, Canada; Hauck *et al.*, 2009) and Ogeechee River estuary (USA; Dörjes & Howard, 1975; Gunn *et al.*, 2007, 2008; Shchepetkina *et al.*, 2016a), in the Mira River estuary, bioturbation intensity, total burrow area and burrow counts increase from the sandier lower estuary to the mud-dominated middle estuary tidal flats.

Energy conditions at the bed might also help explain some of the neoichnological trends, where the interplay between tidal versus fluvial hydraulic energy causes a highly dynamic environment that affects substrate consistency and sediment deposition rates, potentially influencing burrow stability and preservation (Wetzel & Unverricht, 2020). For example, the development and shifting of sandy bars in the lower estuary promote filter feeding over surface and intrastratal deposit feeding (Gingras *et al.*, 2025), resulting in the greater abundance of *Skolithos*, *Scalinichnus*, *Ophiomorpha* and parchment-lined burrows. Moreover, the sandy beds in the lower estuary (Fig. 10) are often massive looking and contain broken bioclasts, reflecting rapid, incremental deposition of event beds that inhibit infaunal colonization. As for the middle estuary, planar parallel laminated beds and those with current ripple lamination (Fig. 9) are frequently non-bioturbated, suggesting the influence of seasonal fluvial floods.

The individual influences of *temperature, oxygenation* and *pH* on the estuarine neoichnological assemblage in the Mira Estuary cannot be distinctly identified and require further experimental studies and detailed analyses to be fully understood. However, as per general guidelines, an increase in *temperature* and its daily and seasonal fluctuations (i.e. temperature stress; La Croix *et al.*, 2022) negatively impacts trace fossil producers, limiting their variability and size, mainly under the coastal upwelling season (April to September). Moreover, temperature stress (both the elevated temperatures during the summer and lower temperature during the winter) increases with tidal flat elevation, leading to a decrease in the number of species and individuals (Johnson, 1965), whereas temperatures low enough to result in ice can lead directly to infaunal mortality and unbioturbated deposits (Yeo & Risk, 1981; Martini & Morrison, 1987; Aitken & Risk, 1988; Wilson, 1990; Martini, 1991; Dale *et al.*, 2002; Dashtgard *et al.*, 2014). Interestingly, a study by Koo *et al.* (2007) revealed that at higher temperatures and thus at higher tidal flat elevations, infauna preferred to construct deep, vertical burrows, seeking refuge from extreme environmental conditions—a trend similar to the one observed in the Mira tidal flats (Fig. 13). Johnson (1965) also mentioned that, unfortunately, the effects of temperature stress on the resultant infauna and traces cannot be easily disentangled from the effects of local climate, water temperature, tidal cycles and type of sediment.

As for the role of *oxygenation*, it is one of the most difficult variables to isolate, with multiple studies devoted to resolving its effects on the resultant ichnocoenoses (Bromley & Ekdale, 1984; Savrda *et al.*, 1984; Martin, 2004; Dashtgard *et al.*, 2015; Dashtgard & MacEachern, 2016). In estuarine environments, the role of oxygenation is closely intertwined with

sediment grain size, salinity and sedimentation rates (MacEachern *et al.*, 2007). According to the current ichnological models, reduced dissolved oxygen levels result in smaller trace sizes, decreased trace abundance and ichnodiversity, shallower tiering and an increase in the number of burrows open to the sediment–water interface (Levin, 2003; Gooday *et al.*, 2010; Dashtgard & Gingras, 2012; Dashtgard *et al.*, 2015; Dashtgard & MacEachern, 2016; La Croix *et al.*, 2022). In contrast, increased oxygen available to burrowing organisms leads to more robust burrows (Gingras *et al.*, 1999), deeper burrow penetration and an increase in subsurface mining (Dashtgard & Gingras, 2012). Normally, oxygenation of water and substrate increases towards the lower estuary and especially in the lower tidal flats due to longer inundation times (Gingras *et al.*, 1999). In contrast, in the Mira River estuary, water oxygenation increases towards the middle estuary (see physico-chemical stresses), likely explaining an insignificant decrease in open burrow diameter as well as the atypical increase in trace diversity landward.

Research on the effects of *pH* on ichnofossil and neoichnological communities is highly limited and entirely lacking for tidal flats, highlighting the need for further studies. However, existing research on major shifts in past ocean pH indicates that increased water acidification can reduce trace fossil abundance and diversity, contributing to mass extinctions (González *et al.*, 2022). In this study, waters in the lower estuary are more alkaline (pH 8.1 to 8.2) compared to the middle estuary (pH 7.7 to 8.0), with pH values in both locations increasing during the high tide. This trend correlates well with salinity values, reflecting mixing between more alkaline ocean water (higher pH and higher salinity) and more acidic fresh water (lower pH and lower salinity). This difference in pH levels may also help explain smaller burrow diameters observed in the upper estuary relative to the lower estuary (Table 2). However, other environmental factors discussed earlier may be more significant in controlling the neoichnological community.

Trace preservation

Preservation potential of traces found in intertidal and supratidal sediments in estuaries primarily depends on the preservation of tidal flats themselves, which is inherently challenging due to their dynamic and often erosional nature (Frey, 1978; Dworschak, 1983; Shchepetkina, 2025). Braat *et al.* (2023) indicated that sediments in estuaries, particularly at higher elevations above the high tide line, have low preservation potential. Only about 40% of these sediments are retained in the rock record, while approximately 60% are subject to reworking, suspension and erosion. Moreover, the intertidal and supratidal flat sediments can be removed by intertidal creeks, ravinement surfaces developed during regional transgression or truncated by channel meandering itself (Reineck & Singh, 1975; Clifton & Phillips, 1980; Yeo & Risk, 1981; Gingras *et al.*, 1999). Middle estuary muddy tidal flats have better chances of preservation because they are harder to erode due to the cohesive nature of mud (Gingras *et al.*, 1999; Shchepetkina *et al.*, 2016c), thus allowing a better preservation of both the shallow and deeper tiers in the rock and sedimentary record. In contrast, lower estuary tidal flats tend to be sandier and are often reworked by meandering channels, thus tending to favour the preservation of only the deepest burrows, with shallower traces eroded (Yeo & Risk, 1981; Gingras *et al.*, 1999). The traces such as *Psilonichnus, Spongeliomorpha*, *Ophiomorpha, Thalassinoides* and 'siphonichnidal burrows' will have the highest preservation potential. They tend to occupy the deepest tiers, that is, can penetrate up to 1 m below the surface of sand and mud tidal flats (Stephenson, 1965; Frey & Mayou, 1971; Seibold *et al.*, 1973; Wetzel & Unverricht, 2020), especially when they are located in more consolidated middle-upper intertidal flat and salt marsh sediments (Allen & Curran, 1974; Frey *et al.*, 1984; Frey & Pemberton, 1987). Shallower- to mid-tier assemblages consisting of *Skolithos-, Arenicolites-, Diplocraterion-*, *Polykladichnus-*, *Palaeophycus-, Lockeia*-like structures and rhizoliths will generally obliterate any structures produced by organisms in the shallowest levels (Ekdale & Bromley, 1991), but have a good chance of preservation, if the substrate is a more cohesive softground to stiffground at some depth below the sediment–water interface. However, with passing time, even the shallower to mid-tier burrows of tidal flats tend to be overprinted, cross-cut or eroded, leading to a higher preservation potential of deepest tiers (Werner & Wetzel, 1982; Ekdale *et al.*, 1984; Frey & Bromley, 1985; Bromley, 1990, 1996; Wetzel, 1991; Buckman, 1996; Dashtgard, 2011a; Mángano & Buatois, 2016; Valencia *et al.*, 2022), thus creating a taphonomic bias.

Surficial traces such as locomotion trackways, trails and general biogenic disturbance represented by traces similar to *Coenobichnus*,

'cruzianaeform', biodeformational structures, cryptic bioturbation and soupground 'swim' traces (Hallam, 1975; Seilacher, 1978; Rindsberg & Kopaska-Merkel, 2013; Muñiz *et al.*, 2015; Belaústegui & Muñiz, 2016; Unno & Semeniuk, 2019) will have the lowest preservation potential, being most easily destroyed by fluvial currents, tidal action, storms, rain splash, deflation at low tide, with only a fraction of surficial traces passing into the rock record (Jensen *et al.*, 2005; Chakrabarti *et al.*, 2006). Droser *et al.* (2002) state that the preservation of shallow-tier traces is essential for accurately determining benthic activity. However, modern tidal flats are highly susceptible to deep sediment mixing, which can obscure or remove these traces, resulting in an artificially diminished representation of the original trace community (Shchepetkina *et al.*, 2023). The only way to preserve delicate surficial traces is the occurrence of rapid sedimentation events, such as storm deposits or waning flood events (Seilacher, 1978; Unno & Semeniuk, 2019). The preservation of surficial traces may also be enhanced when a sharp transition exists between sand and mud layers, effectively sealing off underlying structures from further modification (Seilacher, 1978; Jensen *et al.*, 2005). Other signs of biogenic activity commonly found on the Mira tidal flats that can pass into the record include faecal pellets (microcoprolites). They are often attributed to decapod crustaceans, can serve as biostratigraphic markers (Blau *et al.*, 1993) and are frequently preserved in soft marine sediments, carbonate ramps and deep-sea settings (Senowbari-Daryan & Bernecker, 2005; Peckmann *et al.*, 2007). Despite the pellets often found in surface pits made by fish, burrows of other infauna, flaser beds and in small tidal channels (Yeo & Risk, 1981), their preservation in intertidal settings can be compromised depending on mechanical degradation, reworking or even consumption by other infauna (Rindsberg & Kopaska-Merkel, 2013).

CONCLUSIONS

The neoichnological characteristics of the mesotidal, almost pristine Mira River estuary tidal flats provide insights into smaller scale estuarine systems in the rock and sedimentary record. Our results suggest that various physico-chemical stresses such as salinity, food availability, fluvial influx, subaerial exposure and sediment characteristics (i.e. sediment type and consistency) shape the distribution and diversity of biogenic structures across the tidal flats, creating heterogeneity. The individual influences of temperature, oxygenation, and pH on the estuarine neoichnological assemblage remain unclear and require further experimental studies and detailed analyses to be fully understood.

The middle estuary tidal flats (CBr) are composed of poorly to very poorly sorted silty sand, sandy silt, silt and slightly gravelly muddy sand. They host a moderately to highly diverse neoichnological suite with simple, lined, vertical, inclined to horizontal and Y-shaped burrows. Burrow counts range from 4250 to 6700 burrows/m^2, with minimum and maximum trace diameters of 1.2 to 2 mm and 2 to 3.5 mm, respectively. The suite exhibits a minimum plan view bioturbation intensity of 1 to 2, which was measured solely on vertical and subvertical burrow openings and excluding crab burrows and surface biogenic structures. The vertical bioturbation intensity is sparse to complete (BI 1 to 6), indicating a typical brackish-water suite (i.e. the typical *Teichichnus* Ichnofacies) influenced by strongly fluctuating environmental conditions.

The lower estuary tidal flats (VNMF) are composed of a wider range of coarser-grained sediments including poorly sorted, gravelly medium- to coarse-grained sand, gravelly muddy sand, sandy silt, silty fine- to medium-grained sand and medium-grained sand. These sediments are occupied by a low to high diversity neoichnological assemblage, characterized by low horizontal bioturbation intensity (BI 1), sparse to abundant vertical bioturbation intensity (BI 1 to 5), simple, lined, vertical, inclined to horizontal and Y-shaped burrows, with lower burrow counts (1550 to 3138 burrows/m^2) and larger minimum and maximum trace sizes (2.1 to 2.6 mm and 3.6 to 4.7 mm, respectively). The lower estuary location exhibits increased calcium carbonate content and decreased organic matter content, reflecting the overpowering influence of the nearby ocean.

In the Mira River estuary, bioturbation intensity, total burrow area and open burrow counts increase from the sandy lower estuary to the muddy middle estuary tidal flats, while the trace diversity decreases. This pattern suggests enhanced food availability (higher organic matter %) and finer sediment grains that are conducive to infaunal colonization. However, trace sizes decrease upestuary, indicating escalating physico-chemical stress. The most common traces are produced by vermiform invertebrates (e.g. polychaetes, nemertines, annelids and tube worms), amphipods,

bivalves, crustaceans, fish, and meiofauna, predominantly forming *Skolithos, Arenicolites*, *Diplocraterion*, *Thalassinoides*, *Planolites* and rarely 'siphonichnidal burrows' in the shallower tier and *Palaeophycus, Lockeia, Thalassinoide*s, 'siphonichnidal burrows' and rhizoliths in the deep tier. The potential for trace preservation depends on their position within the substrate (shallow, middle versus deep tiers), the substrate composition (with different trace assemblages preserved in muddy versus sandy substrates), the physical energy of the locale and the overall preservation potential of tidal flats. This study contributes to ongoing efforts to identify facies variability across estuarine tidal flats worldwide and in the geologic record, offering insights into organism communities, depositional environments and physicochemical stress conditions.

ACKNOWLEDGEMENTS

We sincerely thank reviewers Drs. Lynn Dafoe and James MacEachern and Sedimentology editors Drs. Christopher Fielding, Gabriela Mángano, and Marc Aurell for their thoughtful comments and constructive suggestions, which greatly helped improve the clarity and quality of this manuscript. Funding for the research program under which these data were collected and analysed was generously provided by the Portuguese Fundação para a Ciência e a Tecnologia (FCT) I.P./MCTES through national funds (PIDDAC)—UIDB/50019/2020 under the project 'UIDP/50019/2020—Financiamento Plurianual de Unidades de I&D 2020-2023—IDL' and European Multidisciplinary Seafloor and Water-Column Observatory (PINFRA/22157/2016). Additionally, Jacqueline Santos received financial support through grant IPMA-2020-011-BI under the project EMSO-PT and Ana Alberto through PhD grant UIBD/151497/2021 (IDL).

CONFLICT OF INTEREST

All authors declare that they have no conflicts of interest.

DATA AVAILABILITY STATEMENT

The data that support the findings of this study are available from the corresponding author upon reasonable request.

REFERENCES

Adão, H., **Alves, A.S.**, **Patrício, J.**, **Neto, J.M.**, **Costa, M.J.** and **Marques, J.C.** (2009) Spatial distribution of subtidal Nematoda communities along the salinity gradient in southern European estuaries. *Acta Oecologica*, **35**, 287–300.

Aitken, A.E. and **Risk, M.J.** (1988) Animal-sediment relationships on a subarctic intertidal flat, Pangnirtung Fiord, Baffin Island Canada. *SEPM J. Sediment. Res.*, **58**, 969–978.

Alexander, R.R., **Stanton, R.J.** and **Dodd, J.R.** (1993) Influence of sediment grain size on the burrowing of bivalves: correlation with distribution and stratigraphic persistence of selected Neogene clams. *Palaios*, **8**, 289–303.

Allen, E.A. and **Curran, H.A.** (1974) Biogenic sedimentary structures produced by crabs in lagoon margin and salt marsh environments near Beaufort, North Carolina. *J. Sediment. Res.*, **44**, 538–548.

Aller, R.C. (1994) Bioturbation and remineralization of sedimentary organic matter: effects of redox oscillation. *Org. Geochem.*, **114**, 331–345.

Alves, A.S., **Adão, H.**, **Patrício, J.**, **Neto, J.M.**, **Costa, M.J.** and **Marques, J.C.** (2009) Spatial distribution of subtidal meiobenthos along estuarine gradients in two southern European estuaries (Portugal). *J. Marine Biol. Assoc. UK*, **89**, 1529–1540.

Amaral, V., **Queiroga, H.**, **Skov, M.** and **Paula, J.** (2007) Planktonic availability and settlement of *Carcinus maenas* megalopae at high temporal resolution in the lower Mira Estuary (SW Portugal). *Mar. Ecol. Prog. Ser.*, **348**, 239–248.

Austen, M.C. and **Warwick, R.M.** (1989) Comparison of univariate and multivariate aspects of estuarine meiobenthic community structure. *Estuar. Coast. Shelf Sci.*, **29**, 23–42.

Ayranci, K., **Dashtgard, S.E.** and **MacEachern, J.A.** (2014) A quantitative assessment of the neoichnology and biology of a delta front and prodelta, and implications for delta ichnology. *Palaeogeogr. Palaeoclimatol. Palaeoecol.*, **409**, 114–134.

Belaústegui, Z. and **Muñiz, F.** (2016) Ichnology of the Lepe area (Huelva, SW Spain): trace fossils at the Pliocene'Arroyo Valleforero'section and modern traces at the Piedras Estuary. *Comunicações Geológicas*, **103**, 131–142.

Bertling, M., **Braddy, S.**, **Bromley, R.G.**, **Demathieu, G.D.**, **Genise, J.F.**, **Mikuláš, R.**, **Nielsen, J.-K.**, **Nielsen, K.S.S.**, **Rindsberg, A.A.**, **Schlirf, M.** and **Uchman, A.** (2006) Names for trace fossils: a uniform approach. *Lethaia*, **39**, 265–286.

Bertling, M., **Buatois, L.A.**, **Knaust, D.**, **Laing, B.**, **Mángano, M.G.**, **Meyer, N.**, **Mikuláš, R.**, **Minter, N.J.**, **Neumann, C.**, **Rindsberg, A.K.**, **Uchman, A.** and **Wisshak, M.** (2022) Names for trace fossils 2.0: theory and practice in ichnotaxonomy. *Lethaia*, **55**, 1–19.

Bettencourt, A., **Bricker, S.B.**, **Ferreira, J.G.**, **Franco, A.**, **Marques, J.C.**, **Melo, J.J.**, **Nobre, A.**, **Ramos, L.**, **Reis, C.S.**, **Salas, F.**, **Silva, M.C.**, **Simas, T.** and **Wolff, W.J.** (2004) Typology and Reference Conditions for Portuguese Transitional and Coastal Waters (TICOR). *Institute Marine Res.*, **98**, 1216.

Beynon, B.M., **Pemberton, S.G.**, **Bell, D.D.** and **Logan, C.A.** (1988) Environmental implications of ichnofossils from the Lower Cretaceous Grand Rapids Formation, Cold Lake oil

sands deposit. In: *Sequences, Stratigraphy, Sedimentology; Surface and Subsurface* (Eds James, D.P. and Leckie, D.A.), pp. 275–289. CSPG Memoir, Calgary, AB.

Bistran, R. (2014) *Sedimentology and Neoichnology of a Mixed-Energy Estuary, Tillamook Bay, Oregon, United States*. MSc Thesis, p. 385. University of Alberta, Calgary, AB.

Blanton, J.O. and **Andrade, F.A.** (2001) Distortion of tidal currents and the lateral transfer of salt in a shallow coastal plain estuary (O Estuário do Mira, Portugal). *Estuaries*, **24**, 467–480.

Blanton, J.O., **Ferreira, M.A.** and **Andrade, F.A.** (2000) Effect of a broad shallow sill on tidal circulation and salt transport in the entrance to a coastal plain estuary (Mira—Vila Nova de Milfontes, Portugal). *Estuaries*, **23**, 293–304.

Blau, J., **Grün, B.** and **Senff, M.** (1993) Crustaceen-Koprolithen aus der Trias der westlichen Tethys (Lienzer Dolomiten, Österreich; Pragser Dolomiten, Italien) und vom Gondwana-Westrand (oberes Magdalenatal, Kolumbien, Südamerika). *Paläontologische Zeitschrift*, **67**, 193–214.

Blott, S.J. and **Pye, K.** (2012) Particle size scales and classification of sediment types based on particle size distributions: review and recommended procedures. *Sedimentology*, **59**, 2071–2096.

Boggs, S. (2009) *Petrology of Sedimentary Rocks*, p. 612. Cambridge University Press, Cambridge.

Braat, L., **Pierik, H.J.**, **van Dijk, W.M.**, **van de Lageweg, W.I.**, **Brückner, M.Z.**, **van der Meulen, B.** and **Kleinhans, M.G.** (2023) Observed and modelled tidal bar sedimentology reveals preservation bias against mud in estuarine stratigraphy. *Deposit. Record*, **9**, 380–402.

Bromley, R.G. (1990) *Trace Fossils – Biology and Taphonomy*, p. 280. Unwin Hyman, London.

Bromley, R.G. (1996) *Trace Fossils: Biology, Taphonomy and Applications*, p. 361. Chapman and Hall, London.

Bromley, R.G. and **Ekdale, A.A.** (1984) *Chondrites*: a trace fossil indicator of anoxia in sediments. *Science*, **224**, 872–874.

Brown, J., **Colling, A.**, **Park, D.**, **Philips, J.**, **Rothery, D.** and **Wright, J.** (2002a) *Seawater: Its Composition, Properties and Behaviour*, p. 172. The Open University, Milton Keynes.

Brown, J., **Colling, A.**, **Park, D.**, **Philips, J.**, **Rothery, D.** and **Wright, J.** (2002b) *Waves, Tides and Shallow-Water Processes*, p. 187. The Open University, Milton Keynes.

Buatois, L.A., **Gingras, M.K.**, **MacEachern, J.A.**, **Mángano, M.G.**, **Zonneveld, J.-P.**, **Pemberton, S.G.**, **Netto, R.G.** and **Martin, A.** (2005) Colonization of brackish-water systems through time: Evidence from the trace-fossil record. *Palaios*, **20**, 321–347.

Buckman, J.O. (1996) An example of 'deep' tier level *Teichichnus* with vertical entrance shafts from the Carboniferous of Ireland. *Ichnos*, **4**, 241–248.

Castro, P. and **Freitas, H.** (2006) Anthropogenic effects and salt marsh loss in the Mondego and Mira estuaries (Portugal). *Web Ecol.*, **6**, 59–66.

Chakrabarti, A., **Chakrabarti, R.** and **Hertweck, G.** (2006) Surface traces and bioturbate textures from bubbler crabs: an indicator of subtropical to tropical tidal flat environments. *Senckenbergiana maritima*, **36**, 19–27.

Chapman, P.M. (1981) Measurements of the short-term stability of interstitial salinities in subtidal estuarine sediments. *Estuar. Coast. Shelf Sci.*, **12**, 67–81.

Clifton, H.E. and **Phillips, R.L.** (1980) Lateral trends and vertical sequences in estuarine sediments, Willapa Bay, Washington. In: *Proceedings of the Quaternary Depositional Environments of the Pacific Coast* (Eds Field, M.E., Bouma, A.H., Colburn, I.P., Douglas, R. and Ingle, J.C.), *Pacific Coast Paleogeography Symposium*, **4**, 55–71.

Costa, M.J., **Catarino, F.** and **Bettencourt, A.** (2001) The role of salt marshes in the Mira estuary (Portugal). *Wetlands Ecol. Manag.*, **9**, 121–134.

Croghan, P.C. (1976) Ionic and osmotic regulation of aquatic animals. In: *Environmental Physiology of Animals* (Eds Bligh, J., Cloudsley-Thompson, J.L. and MacDonald, A.G.). Blackwell, Oxford.

Dale, J.E., **Leech, S.**, **McCann, S.B.** and **Samuelson, G.** (2002) Sedimentary characteristics, biological zonation and physical processes of the tidal flats of Iqaluit, Nunavut. In: *Landscapes of Transition* (Eds Hewitt, K., Byrne, M.-L., English, M. and Young, G.), pp. 205–234. The GeoJournal Library, Springer, Dordrecht.

Dashtgard, S.E. (2011a) Linking invertebrate burrow distributions (neoichnology) to physicochemical stresses on a sandy tidal flat: Implications for the rock record. *Sedimentology*, **58**, 1303–1325.

Dashtgard, S.E. (2011b) Neoichnology of the lower delta plain: Fraser River Delta, British Columbia, Canada: Implications for the ichnology of deltas. *Palaegeogr. Palaeoclimatol. Palaeoecol.*, **307**, 98–108.

Dashtgard, S.E. and **Gingras, M.K.** (2012) Marine invertebrate neoichnology. In: *Trace Fossils as Indicators of Sedimentary Environments* (Eds Knaust, D. and Bromley, R.G.), pp. 273–295. Elsevier, London.

Dashtgard, S.E. and **MacEachern, J.A.** (2016) Unburrowed mudstones may record only slightly lowered oxygen conditions in warm, shallow basins. *Geology*, **44**, 371–374.

Dashtgard, S.E., **Gingras, M.K.** and **Pemberton, S.G.** (2008) Grain-size controls on the occurrence of bioturbation. *Palaeogeogr. Palaeoclimatol. Palaeoecol.*, **257**, 224–243.

Dashtgard, S.E., **Pearson, N.J.** and **Gingras, M.K.** (2014) Sedimentology, ichnology, ecology and anthropogenic modification of muddy tidal flats in a cold-temperate environment: Chignecto Bay, Canada. In: *Sedimentary Coastal Zones from High to Low Latitudes: Similarities and Differences* (Ed. Dashtgard, S.E.), pp. 229–245. Geological Society of London, Special Publications, London.

Dashtgard, S.E., **Snedden, J.W.** and **MacEachern, J.A.** (2015) Unbioturbated sediments on a muddy shelf: Hypoxia or simply reduced oxygen saturation? *Palaeogeogr. Palaeoclimatol. Palaeoecol.*, **425**, 128–138.

Dörjes, J. and **Howard, J.D.** (1975) Estuaries of the Georgia Coast, USA: Sedimentology and biology. IV. Fluvial-marine transition indicators in an estuarine environment, Ogeechee River-Ossabaw Sound. In: *Estuaries of the Georgia Coast, U.S.A.: Sedimentology and Biology* (Eds Hertweck, G. and Little-Gadow, S.), pp. 137–179. Senckenbergische Naturforschende Gesellschaft, Frankfurt.

Downing, A.L. and **Truesdale, G.A.** (1955) Some factors affecting the rate of solution of oxygen in water. *J. Appl. Chem.*, **5**, 570–581.

Droser, M.L., **Jensen, S.** and **Gehling, J.G.** (2002) Trace fossils and substrates of the terminal Proterozoic-Cambrian transition: Implications for the record of early bilaterians and sediment mixing. *Proc. Natl. Acad. Sci.*, **99**, 12572–12576.

Duarte, B., **Manjate, E.** and **Caçador, I.** (2020) Baseline survey on the accumulation of microdebris in the intertidal sediments of a reference estuarine system (Mira estuary, Portugal). *Oceans*, **1**, 47–55.

Dworschak, P.C. (1983) The biology of *Upogebia pusilla* (Petagna) (Decapoda, Thalassinidea) I. the burrows. *Marine Ecol.*, **4**, 19–43.

Ekdale, A.A. (1985) Paleoecology of the marine endobenthos. *Palaeogeogr. Palaeoclimatol. Palaeoecol.*, **50**, 63–81.

Ekdale, A.A. and **Bromley, R.G.** (1991) Analysis of composite ichnofabrics: an example in uppermost Cretaceous chalk of Denmark. *Palaios*, **6**, 232–249.

Ekdale, A.A., **Bromley, R.G.** and **Pemberton, S.G.** (1984) *Ichnology: The Use of Trace Fossils in Sedimentology and Stratigraphy, SEPM Short Course Notes, 15*, p. 317. Society of Economic Paleontologists and Mineralogists, Tulsa, OK.

Elders, C.A. (1975) Experimental approaches in neoichnology. In: *The Study of Trace Fossils: A Synthesis of Principles, Problems, and Procedures in Ichnology* (Ed. Frey, R.W.), pp. 513–536. Springer-Verlag, New York, NY.

Eltom, H.A., **Alqubalee, A.M.** and **Babalola, L.O.** (2022) Understanding the two-dimensional quantification of bioturbation intensity through computer modeling and statistical analysis. *Int. J. Earth Sci.*, **111**, 127–143.

Fatela, F., **Moreno, J.** and **Cabral, M.C.** (2016) Salinity and water temperature assessment of the tidal marshes from the W Portuguese coast, as an ecological tool to palaeoenvironmental reconstructions based on foraminifera and ostracoda assemblages. *Estudos do Quaternario*, **14**, 73–81.

Felder, D.L. (1978) Osmotic and ionic regulation in several Western Atlantic Callianassidae (Crustacea, Decapoda, Thalassinidea). *Biol. Bull.*, **154**, 409–429.

Ferreira, J.G., **Simas, T.**, **Nobre, A.**, **Silva, M.C.**, **Shifferegger, K.** and **Lencart-Silva, J.** (2003) Identification of sensitive areas and vulnerable zones in transitional and coastal Portuguese systems. In: *Application of the United States National Estuarine Eutrophication Assessment to the Minho, Lima, Douro, Ria de Aveiro, Mondego, Tagus, Sado, Mira, Ria Formosa and Guadiana Systems*. Instituto da Água e Instituto do Mar, Lisboa, Portugal.

Fiúza, A. (1983) Upwelling patterns off Portugal. In: *Coastal Upwelling. Its Sediment Record* (Eds Suess, E. and Thiede, J.), pp. 85–98. Plenum, New York, NY.

Folk, R.L. (1954) The distinction between grain size and mineral composition in sedimentary-rock nomenclature. *J. Geol.*, **62**, 344–359.

Folk, R.L. (1966) A review of grain size parameters. *Sedimentology*, **6**, 73–93.

Folk, R.L. and **Ward, W.C.** (1957) Brazos River bar [Texas]: A study in the significance of grain size parameters. *J. Sediment. Res.*, **27**, 3–26.

Frey, R.W. (1978) Behavioral and ecological implications of trace fossils. In: *Trace Fossil Concepts, SEPM Short Course* (Ed. Basan, P.B.), pp. 43–66. Society of Economic Paleontologists and Mineralogists, Tulsa, OK.

Frey, R.W. and **Bromley, R.G.** (1985) Ichnology of American chalks: the Selma Group (Upper Cretaceous), western Alabama. *Can. J. Earth Sci.*, **22**, 801–828.

Frey, R.W. and **Mayou, T.V.** (1971) Decapod burrows in Holocene barrier Island beaches and washover fans, Georgia. *Senckenbergiana Maritima*, **3**, 53–77.

Frey, R.W. and **Pemberton, S.G.** (1987) The *Psilonichnus* ichnocoenose, and its relationship to adjacent marine and nonmarine ichnocoenoses along the Georgia coast. *Bull. Canadian Petrol. Geol.*, **35**, 333–357.

Frey, R.W., **Curran, H.A.** and **Pemberton, S.G.** (1984) Tracemaking activities of crabs and their environmental significance: the ichnogenus *Psilonichnus*. *J. Paleo.*, **58**, 333–350.

Gingras, M.K. and **Bann, K.L.** (2006) The bend justifies the leans: interpreting recumbent ichnofabrics. *J. Sediment. Res.*, **76**, 483–492.

Gingras, M.K., **Pemberton, S.G.**, **Saunders, T.D.A.** and **Clifton, H.E.** (1999) The ichnology of modern and Pleisorganic matterene brackish-water deposits at Willapa Bay, Washington: variability in estuarine settings. *Palaios*, **14**, 352–374.

Gingras, M.K., **Pemberton, S.G.** and **Saunders, T.** (2000) Firmness profiles associated with tidal-creek deposits: the temporal significance of Glossifungites assemblages. *J. Sediment. Res.*, **70**, 1017–1025.

Gingras, M.K., **Pickerrill, R.** and **Pemberton, G.S.** (2002a) Resin cast of modern burrows provides analogs for composite trace fossils. *Palaios*, **17**, 206–211.

Gingras, M.K., **Rasanen, M.** and **Ranzi, A.** (2002b) The significance of bioturbated Inclined Heterolithic Stratification in the southern part of the Miocene Solimoes Formation, Rio Acre, Amazonia Brazil. *Palaios*, **17**, 591–601.

Gingras, M.K., **Bann, K.L.**, **MacEachern, J.A.** and **Pemberton, S.G.** (2007) A conceptual framework for the application of trace fossils. In: *Applied Ichnology* (Eds MacEachern, J.A., Bann, K.L., Gingras, M.K. and Pemberton, S.G.), pp. 1–26. Society of Economic Paleontologists and Mineralogists, Tulsa, OK.

Gingras, M.K., **MacEachern, J.A.** and **Dashtgard, S.E.** (2011) Process ichnology and the elucidation of physico-chemical stress. *Sediment. Geol.*, **237**, 115–134.

Gingras, M.K., **MacEachern, J.A.**, **Dashtgard, S.E.**, **Zonneveld, J.-P.**, **Schoengut, J.A.**, **Ranger, M.J.** and **Pemberton, S.G.** (2012) Estuaries. In: *Trace Fossils as Indicators of Sedimentary Environments* (Eds Knaust, D. and Bromley, R.G.), pp. 463–505. Elsevier BV, London.

Gingras, M.K., **Zonneveld, J.** and **Konhauser, K.O.** (2014) Experimental Approaches to Understanding Fossil Organisms. In: *Experimental Approaches to Understanding Fossil Organisms: Lessons from the Living* (Eds Hembree, D.I., Platt, B.F. and Smith, J.J.), pp. 195–206. Springer Science+Business Media, Dordrecht.

Gingras, M.K., **MacEachern, J.A.**, **Dashtgard, S.E.** and **Bann, K.L.** (2025) The Teichichnus Ichnofacies: Its neoichnological basis and identification in the rock record. *Sedimentology*, **72**, 408–441.

González, P.D., **Furlong, C.M.**, **Gingras, M.K.**, **Playter, T.** and **Zonneveld, J.P.** (2022) Depositional framework and trace fossil assemblages of the lower Triassic Montney formation, northeastern British Columbia, Western Canada Sedimentary Basin. *Marine Petrol. Geol.*, **143**, 105822.

Gooday, A.J., **Bett, B.J.**, **Escobar, E.**, **Ingole, B.**, **Levin, L.A.**, **Neira, C.**, **Raman, A.V.** and **Sellanes, J.** (2010) Habitat heterogeneity and its influence on benthic biodiversity in oxygen minimum zones. *Marine Ecol.*, **31**, 125–147.

Grassle, J.F. and **Grassle, J.P.** (1974) Opportunistic life histories and genetic systems in marine benthic polychaetes. *J. Mar. Res.*, **32**, 253–284.

Greb, S.F. and **Chesnut, D.R.** (1994) Paleoecology of an estuarine sequence in the Breathitt Formation (Pennsylvanian), Central Appalachian Basin. *Palaios*, **9**, 388–402.

Gunn, S.C., **Dalrymple, R.W.**, **Pemberton, S.G.** and **Gingras, M.K.** (2007) Facies Variability of Tidal Bar Occurrences in a Tidal-Fluvial Transition One, Ogeechee Estuary, Georgia, U.S.A. Abstracts: Annual Meeting — American Association of Petroleum Geologists, 57–58.

Gunn, S.C., **Gingras, M.K.**, **Dalrymple, R.W.** and **Pemberton, S.G.** (2008) Ichnological gradation of subtidal deposits, Ogeechee Estuary, Georgia, USA. AAPG Search and Discover Article #90078. Annual Meeting — American Association of Petroleum Geologists.

Hallam, A. (1975) Preservation of trace fossils. In: *The Study of Trace Fossils: A Synthesis of Principles, Problems, and Procedures in Ichnology*, pp. 55–63. Springer Berlin Heidelberg, Berlin, Heidelberg.

Häntzschel, W. (1939) Tidal flat deposits (Wattenschlick). In: *Recent Marine Sediments* (Ed. Trask, P.D.), pp. 195–206. American Association of Petroleum Geologists, Tulsa, OK.

Hauck, T.E. (2008) *Sedimentology and Ichnology of a Wave-Dominated, Microtidal Barrier Island/Embayment System, New Brunswick, Canada*, p. 134. Univeristy of Alberta, Edmonton, AB.

Hauck, T.E., **Dashtgard, S.E.**, **Pemberton, S.G.** and **Gingras, M.K.** (2009) Brackish-water ichnological trends in a microtidal barrier Island-embayment system, Kouchibouguac National Park, New Brunswick, Canada. *Palaios*, **24**, 478–496.

Heckel, P.H. (1972) Recognition of ancient shallow marine environments. In: *Recognition of Ancient Sedimentary Environments* (Eds Rigby, J.K. and Hamblin, W.K.), pp. 226–286. SEPM (Society for Sedimentary Geology), Tulsa, OK.

Heip, C.H.R., **Vincx, M.** and **Vranken, G.** (1985) The ecology of marine nematodes. *Oceanogr. Marine Biol. Ann. Rev.*, **23**, 399–489.

Heiri, O., **Lotter, A.F.** and **Lemcke, G.** (2001) Loss on ignition as a method for estimating organic and carbonate content in sediments: reproducibility and comparability of results. *J. Paleo.*, **25**, 101–110.

Hovikoski, J., **Gingras, M.**, **Räsänen, M.**, **Rebata, L.A.**, **Guerrero, J.**, **Ranzi, A.**, **Melo, J.**, **Romero, L.** and **Lopez, S.** (2007) The nature of Miocene Amazonian epicontinental embayment: high-frequency shifts of the low-gradient coastline. *Geol. Soc. Am. Bull.*, **119**, 1506–1520.

Howard, J.D. (1975) The sedimentological significance of trace fossils. In: *The Study of Trace Fossils: A Synthesis of Principles, Problems, and Procedures in Ichnology*, pp. 131–146. Springer-Verlag, New York, NY.

Howard, J.D. and **Frey, R.W.** (1975) Regional animal-sediment characteristics of Georgia estuaries. In: *Estuaries of the Georgia Coast, U.S.A.: Sedimentology and Biology* (Eds Hertweck, G. and Little-Gadow, S.), pp. 33–103. Senckenbergische Naturforschende Gesellschaft, Frankfurt.

Howard, J.D., **Elders, C.A.** and **Heinbokel, J.F.** (1975) Animal-sediment relationships in estuarine point bar deposits, Ogeechee River-Ossabaw Sound, Georgia. In: *Estuaries of the Georgia Coast, U.S.A.: Sedimentology and Biology* (Eds Hertweck, G. and Little-Gadow, S.), pp. 181–203. Senckenbergische Naturforschende Gesellschaft, Frankfurt.

Jensen, S., **Droser, M.L.** and **Gehling, J.G.** (2005) Trace fossil preservation and the early evolution of animals. *Palaeogeogr. Palaeoclimatol. Palaeoecol.*, **220**, 19–29.

Johnson, R.G. (1965) Temperature variation in the infaunal environment of a sand flat. *Limnol. Oceanogr.*, **10**, 114–120.

Knaust, D. (2015) *Siphonichnidae* (new ichnofamily) attributed to the burrowing activity of bivalves: ichnotaxonomy, behaviour and palaeoenvironmental implications. *Earth-Sci. Rev.*, **150**, 497–519.

Knaust, D. (2020) Invertebrate coprolites and cololites revised. *Pap. Palaeontol.*, **6**, 385–423.

Koo, B.J., **Kwon, K.K.** and **Hyun, J.H.** (2007) Effect of environmental conditions on variation in the sediment-water interface created by complex macrofaunal burrows on a tidal flat. *J. Sea Res.*, **58**, 302–312.

Kretzschmar, R. (1991) *Kulturtechnisch-bodenkundliches Praktikum. Ausgewählte Laboratoriumsmethoden.* Aufl. Selbstverlag, Univ, Kiel.

Krumbein, W.C. and **Pettijohn, F.J.** (1938) *Manual of Sedimentary Petrography*, p. 549. Appleton-Century-Crofts, New York, NY.

La Croix, A.D. and **Dashtgard, S.E.** (2015) A synthesis of depositional trends in intertidal and upper subtidal sediments across the tidal–fluvial transition in the Fraser River, Canada. *J. Sediment. Res.*, **85**, 683–698.

La Croix, A.D., **Dashtgard, S.E.**, **Gingras, M.K.**, **Hauck, T.E.** and **MacEachern, J.A.** (2015) Bioturbation trends across the freshwater to brackish-water transition in rivers. *Palaeogeogr. Palaeoclimatol. Palaeoecol.*, **440**, 66–77.

La Croix, A.D., **Ayranci, K.** and **Dashtgard, S.E.** (2022) Neoichnology of siliciclastic shallow-marine environments: Invertebrates, traces, and environmental conditions. *Earth-Sci. Rev.*, **233**, 104170.

Lettley, C.D., **Gingras, M.K.**, **Pearon, N.J.** and **Pemberton, S.G.** (2007) Burrowed stiffgrounds on estuarine point bars: modern and ancient examples, and criteria for their discrimination from firmgrounds developed along omission surfaces. In: *Applied Ichnology* (Eds MacEachern, J.A., Bann, K.L., Gingras, M.K. and Pemberton, S.G.), pp. 317–325. SEPM (Society for Sedimentary Geology), Short Course Note 52, Tulsa, USA.

Levin, L.A. (2003) Oxygen minimum zone bethos: adaptation and community response to hypoxia. *Oceanogr. Marine Biol. Ann. Rev.*, **41**, 1–45.

Lobza, V. and **Schieber, J.** (1999) Biogenic sedimentary structures produced by worms in soupy, soft muds; observations from the Chattanooga Shale (Upper Devonian) and experiments. *J. Sediment. Res.*, **69**, 1041–1049.

Luternauer, J.L., **Atkins, R.J.**, **Moody, A.I.**, **Williams, H.F.L.** and **Gibson, J.W.** (1995) Salt Marshes. In: *Geomorphology and Sedimentology of Estuaries* (Ed. Perillo, G.M.E.), pp. 307–332. Elsevier Science, London.

MacEachern, J.A. and **Gingras, M.K.** (2007) Recognition of brackish-water trace-fossil suites in the Cretaceous Western Interior Seaway of Alberta, Canada. In: *Sediment-Organism Interactions; A Multifaceted Ichnology* (Eds Bromley, R.G., Buatois, L.A., Mángano, M.G., Genise, J.F. and Melchor, R.N.), pp. 149–193. Special Publication - SEPM, Tulsa, OK.

Maceachern, J.A. and **Pemberton, S.G.** (1994) Ichnological aspects of incised-valley fill systems from the Viking Formation of the Western Canada Sedimentary Basin, Alberta, Canada. In: *Incised-Valley Systems: Origin and Sedimentary Sequences* (Eds Dalrymple, R.W., Zaitlin, B.A. and Scholle, P.A.), *SEPM Spec. Pub*, **5**, 129–157.

MacEachern, J.A., **Pemberton, S.G.**, **Bann, K.L.** and **Gingras, M.K.** (2007) Departures from the archetypal ichnofacies: effective recognition of physico-chemical stresses in the rock record. In: *Applied Ichnology* (Eds MacEachern, J.A., Bann, K.L., Gingras, M.K. and Pemberton, S.G.), pp. 65–93. SEPM, Short Course Notes No. 52, Tulsa, OK.

MacEachern, J.A., **Bann, K.L.**, **Gingras, M.K.**, **Zonneveld, J.P.**, **Dashtgard, S.E.** and **Pemberton, S.G.** (2012) The ichnofacies paradigm. In: *Trace Fossils as Indicators of Sedimentary Environments* (Eds Knaust, D. and Bromley, R.G.), pp. 103–138. Elsevier, Amsterdam.

Mángano, M.G. and **Buatois, L.A.** (2016) *The Trace-Fossil Record of Major Evolutionary Events. Mesozoic and Cenozoic*, p. 372. Springer Science+Business Media, Dordrecht, Berlin.

Marenco, K.N. and **Bottjer, D.J.** (2010) The intersection grid technique for quantifying the extent of bioturbation on bedding planes. *Palaios*, **25**, 457–462.

Martin, K.D. (2004) A re-evaluation of the relationship between trace fossils and dysoxia. In: *The Application of Ichnology to Palaeoenvironmental and Stratigraphic Analysis* (Ed. McIlroy, D.), pp. 141–156. Geological Society of London, Special Publication No. 228, London.

Martini, I.P. (1991) Sedimentology of subarctic tidal flats in western James Bay and Hudson Bay, Ontario, Canada. In: *Tidal Sedimentology 16* (Eds Smith, D.G., Reinson, G.E., Zaitlin, B.A. and Rahmani, R.A.), pp. 301–312. Canadian Association of Petroleum Geologists, Calgary.

Martini, I.P. and **Morrison, R.I.G.** (1987) Regional distribution of Macoma balthica and Hydrobia minuta on the subarctic coasts of Hudson Bay and James Bay, Ontario. *Estuar. Coastal Shelf Sci.*, **24**, 47–68.

Martins, L.R. (1965) Significance of skewness and kurtosis in environmental interpretation. *J. Sediment. Res.*, **35**, 768–770.

Mason, C.C. and **Folk, R.L.** (1958) Differentiation of Beach, Dune, and Aeolian Flat Environments by Size Analysis, Mustang Island, Texas. *SEPM J. Sediment. Res.*, **28**, 211–226.

Matos, I. (2008) Plano de Ordenamento do Parque Natural do Sudoeste Alentejano e Costa Vicentina. Avaliação Ambiental Estratégica. Relatório Ambiental. Estudos De Base. Etapa 1 – Descrição Volume I /III. Ministério do Ambiente, Ordenamento do Terratório e Desenvolvimento Regional, 42 pp.

McIlroy, D. (2004) The application of ichnology to palaeoenvironmental and stratigraphic analysis: Introduction. *Geol. Soc. Lond. Spec. Publ.*, **228**, 1–2.

Medeiros, J.P., **Chaves, M.L.**, **Silva, G.**, **Azeda, C.**, **Costa, J.L.**, **Marques, J.C.**, **Costa, M.J.** and **Chainho, P.** (2012) Benthic condition in low salinity areas of the Mira estuary (Portugal): Lessons learnt from freshwater and marine assessment tools. *Ecol. Indic.*, **19**, 79–88.

Melnyk, S., **Coutret, B.**, **Brown, D.**, **Zonneveld, J.P.**, **Kavanaugh, J.L.** and **Gingras, M.K.** (2025) Assessing vertical bioturbation intensity from bedding planes. *Geol. Soc. Lond. Spec. Publ.*, **556**, SP556-2024.

Moens, T. and **Vincx, M.** (2000) Temperature and salinity constraints on the life cycle of two brackish-water nematode species. *J. Exp. Mar. Biol. Ecol.*, **243**, 115–135.

Moreno, J., **Fatela, F.**, **Leorri, E.**, **Moreno, F.**, **Freitas, M.C.**, **Valente, T.**, **Araújo, M.F.**, **Gómez-Navarro, J.J.**, **Guise, L.** and **Blake, W.H.** (2017) Bromine soil/sediment enrichment in tidal salt marshes as a potential indicator of climate changes driven by solar activity: New insights from W coast Portuguese estuaries. *Sci. Total Environ.*, **580**, 324–338.

Moreno, J., **Fatela, F.**, **Leorri, E.**, **Gonçalves, M.A.**, **Gómez-Navarro, J.J.**, **Araújo, M.F.**, **Freitas, M.C.**, **Trigo, R.M.**, **Blake, W.H.** and **Moreno, F.** (2019) Foraminiferal evidence of major environmental changes driven by the sun-climate coupling in the western Portuguese coast (14th century to present). *Estuar. Coast. Shelf Sci.*, **218**, 106–118.

Moutzouris, C.I. and **Daniil, E.I.** (1995) Water oxygenation in the vicinity of coastal structures due to wave breaking. In: *Coastal Engineering 1994* (Ed Edge, B.L.), pp. 3167–3177. American Society of Civil Engineers, New York.

Muñiz, F., **Belaústegui, Z.**, **Cárcamo, C.**, **Domènech, R.** and **Martinell, J.** (2015) *Cruziana*-and *Rusophycus*-like traces of recent Sparidae fish in the estuary of the Piedras River (Lepe, Huelva, SW Spain). *Palaeogeogr. Palaeoclimatol. Palaeoecol.*, **439**, 176–183.

Passega, R. (1964) Grain size representation by CM patterns as a geologic tool. *J. Sediment. Res.*, **34**, 830–847.

Paula, J. (1998) Larval retention and dynamics of the prawns *Palaemon longirostris* H. Milne Edwards and *Crangon crangon* Linnaeus (Decapoda, Caridea) in the Mira estuary. *Portugal Invert. Reprod. Develop.*, **33**, 221–228.

Paula, J., **Silva, I.C.**, **Francisco, S.M.** and **Flores, A.V.** (2006) The use of artificial benthic collectors for assessment of spatial patterns of settlement of megalopae of *Carcinus maenas* (L.) (Brachyura: Portunidae) in the lower Mira Estuary, Portugal. *Hydrobiology*, **557**, 69–77.

Pearson, N.J. (2006) *A Sedimentologic and Ichnologic Facies Model for Mud-Dominated Inner-Estuarine Deposits, Mary's Point and the Shepody River, Bay of Fundy, New Brunswick, Canada*, p. 126. University of Alberta, Edmonton, AB.

Pearson, N.J. and **Gingras, M.K.** (2006) An ichnological and sedimentological facies model for muddy point-bar deposits. *J. Sediment. Res.*, **76**, 771–782.

Peckmann, J., **Senowbari-Daryan, B.**, **Birgel, D.** and **Goedert, J.L.** (2007) The crustacean ichnofossil Palaxius associated with callianassid body fossils in an Eocene methane-seep limestone, Humptulips Formation, Olympic Peninsula, Washington. *Lethaia*, **40**, 273–280.

Pemberton, S.G. and **Wightman, D.M.** (1992) Ichnological characteristics of brackish water deposits. In: *Applications of Ichnology to Petroleum Exploration. SEPM Core Workshop Notes No. 17* (Ed. Pemberton, S.G.), pp. 141–167. SEPM (Society for Sedimentary Geology), Tulsa, OK.

Pemberton, S.G., **Flach, P.D.** and **Mossop, G.D.** (1982) Trace fossils from the Athabasca Oil Sands, Alberta, Canada. *Science, New Series*, **217**, 825–827.

Pequeux, A. (1995) Osmotic regulation in crustaceans. *J. Crustacean Biol.*, **15**, 1–60.

Picado, A., **Mendes, J.**, **Ruela, R.**, **Pinheiro, J.** and **Dias, J.M.** (2020) Physico-chemical characterization of two portuguese coastal systems: Ria de Alvor and Mira estuary. *J Mar Sci Eng*, **8**, 537–559.

Ré, P. (1996) Anchovy spawning in the Mira estuary (southwestern Portugal). *Scientia Marina (Espana)*, **60**, 141–153.

Reineck, H.-E. (1963) Sedimentgefüge im Bereich der südlichen Nordsee. *Abhandlungen der Senckenbergischen Naturforschenden Gesellschaft, Band*, **505**, 138.

Reineck, H.-E. and **Singh, I.B.** (1975) *Depositional Sedimentary Environments*, pp. 355–371. Springer-Verlag, New York, NY.

Relvas, P., **Barton, E.D.**, **Dubert, J.**, **Oliveira, P.B.**, **Peliz, Á.**, **Silva, J.C.B.**, **Miguel, A.** and **Santos, A.** (2007) Physical oceanography of the western Iberia ecosystem: Latest views and challenges. *Prog. Oceanogr.*, **74**, 149–173.

Remane, A. and **Schlieper, C.** (1971) *Biology of Brackish Water*, p. 372. John Wiley and Sons, New York, NY.

Ribaudo, C., **Tison-Rosebery, J.**, **Eon, M.**, **Jan, G.** and **Bertrin, V.** (2021) Wind exposure regulates water oxygenation in densely vegetated shallow lakes. *Plants*, **10**, 1269.

Richter, R. (1920) Flachseebeobachtungen I. Ein devonischer 'Pfeifenquazit' verglichen mit der heutigen 'Sandkoralle' (Sabellaria, Ann.). *Senckenbergiana*, **2**, 215–235.

Rindsberg, A.K. and **Kopaska-Merkel, D.C.** (2013) Paleoecology and diagenesis of *Parafavreina ziczac* isp. nov., a crustacean microcoprolite from the Upper Jurassic (Oxfordian) Smackover Formation of Alabama. *Bull. Alabama Mus. Natural His.*, **31**, 74–93.

Sahu, B.K. (1964) Depositional mechanisms from the size analysis of clastic sediments. *J. Sediment. Petrol.*, **34**, 73–83.

Savrda, C.E., **Bottjer, D.J.** and **Gorsline, D.S.** (1984) Development of a comprehensive oxygen-deficient marine biofacies model: evidence from Santa Monica, San Pedro, and Santa Barbara Basins, California Continental Borderland. *AAPG Bulletin*, **68**, 1179–1192.

Schäfer, W. (1972) *Ecology and Paleoecology of Marine Environments*, p. 607. Oliver and Boyd, Edinburgh.

Schoengut, J.A. (2011) *Sedimentological and Ichnological Characteristics of Modern and Ancient Channel-Fills, Willapa Bay, Washington*. MSc Thesis, p. 230. University of Alberta, Edmonton, AB.

Seibold, E., **Diester, L.**, **Fütterer, D.**, **Lange, H.**, **Müller, P.** and **Werner, F.** (1973) Holocene sediments and sedimentary processes in the Iranian part of the Persian Gulf. In: *The Persian Gulf: Holocene Carbonate Sedimentation and Diagenesis in a Shallow Epicontinental Sea* (Ed. Purser, B.H.), pp. 57–80. Springer, Berlin, Heidelberg.

Seilacher, A. (1978) Use of trace fossil assemblages for recognizing depositional environments. *Trace Fossil Concepts, SEPM Short Course*, **5**, 167–181.

Senowbari-Daryan, B. and **Bernecker, M.** (2005) Crustacean coprolites of the late Triassic Tethys: biogeography from the Mediterranian to the middle East. *J. Alpine Geol.*, **47**, 137–144.

Shchepetkina, A. (2025) Crab traces on muddy tidal flats of the Mira River estuary, Portugal. *Palaios*, **40**, 19–34.

Shchepetkina, A., **Gingras, M.K.** and **Pemberton, S.G.** (2016a) Sedimentology and ichnology of the fluvial reach to inner estuary of the Ogeechee River estuary, Georgia, USA. *Sediment. Geol.*, **342**, 202–217.

Shchepetkina, A., **Gingras, M.K.**, **Pemberton, S.G.** and **MacEachern, J.A.** (2016b) What does the ichnological content of the Middle McMurray Formation tell us? *Bull. Canadian Petrol. Geol.*, **64**, 24–46.

Shchepetkina, A., **Gingras, M.K.** and **Pemberton, S.G.** (2016c) Sedimentary fabrics of the macrotidal, mud-dominated, inner estuary to fluvio-tidal transition zone, Petitcodiac River estuary, New Brunswick, Canada. *Sediment. Geol.*, **333**, 147–163.

Shchepetkina, A., **Drago, T.**, **Santos, J.**, **Alberto, A.**, **Shchepetkina, A.**, **Drago, T.**, **Santos, J.** and **Alberto, A.** (2023) Effects of X-ray computed tomography (CT) on the ichnologic interpretation of the Mira River estuary sediment core, SW Portugal. *Ichnos*, **20**, 1–14.

Solárzano, E.J., **Buatois, L.A.**, **Rodrıguez, W.J.** and **Mángano, M.G.** (2017) From freshwater to fully marine: Exploring animal-substrate interactions along a salinity gradient (Miocene Oficina Formation of Venezuela). *Palaeogeogr. Palaeoclimatol. Palaeoecol.*, **482**, 30–47.

Stanistreet, I.G., **Smith, L.B.**, **G.** and **Cadle, A.B.** (1980) Trace fossils as sedimentological and palaeoenvironmental indices in the Ecca Group (Lower Permian) of the Transvaal. *South Afr J. Geol.*, **83**, 333–344.

Stephenson, D.G. (1965) Fossil burrows on the coast of Kenya. *Nature*, **85**, 850–851.

Steyaert, M., **Vanaverbeke, J.**, **Vanreusel, A.**, **Barranguet, C.**, **Lucas, C.** and **Vincx, M.** (2003) The importance of fine-scale, vertical profiles in characterising nematode community structure. *Estuar. Coast. Shelf Sci.*, **58**, 353–366.

Swinbanks, D.D. (1981) Sediment reworking and the biogenic formation of clay laminae by Abarenicola pacifica. *J. Sediment. Petrol.*, **51**, 1137–1145.

Swinbanks, D.D. and **Luternauer, J.L.** (1987) Burrow distribution of Thalassinidean shrimp on a Fraser Delta tidal flat, British Columbia. *J. Paleo.*, **61**, 315–332.

Swinbanks, D.D. and **Murray, J.W.** (1981) Biosedimentological zonation of Boundary Bay tidal flats, Fraser River Delta, British Columbia. *Sedimentology*, **28**, 201–237.

Taylor, A.M. and **Goldring, R.** (1993) Description and analysis of bioturbation and ichnofabric. *J. Geol. Soc. London*, **150**, 141–148.

Unno, J. and **Semeniuk, V.** (2019) Soldier crab paleo-ichnology and its preservation in beach rock along the Pilbara Coast, Western Australia: its geoheritage significance. *Aust. J. Earth Sci.*, **66**, 923–935.

Valencia, F.L., **Mángano, M.G.**, **Buatois, L.A.** and **Laya, J.C.** (2022) Animal–substrate interactions preserved in ancient lagoonal chalk. *Sci. Rep.*, **12**, 14383.

Vinagre, C., **Cabral, H.N.** and **Costa, M.J.** (2010) Relative importance of estuarine nurseries for species of the genus Diplodus (Sparidae) along the Portuguese coast. *Estuar. Coast. Shelf Sci.*, **86**, 197–202.

Werner, F. and **Wetzel, A.** (1982) Interpretation of biogenic structures in oceanic sediments. *Bull. Institute Géologique du Bassin d'Aquitaine*, **31**, 2548.

Wetzel, A. (1991) Ecologic interpretation of deep-sea trace fossil communities. *Palaeogeogr. Palaeoclimatol. Palaeoecol.*, **85**, 47–69.

Wetzel, A. and **Unverricht, D.** (2020) Sediment dynamics of estuarine Holocene incised-valley fill deposits recorded by *Siphonichnus* (ancient Red River, Gulf of Tonkin). *Palaeogeogr. Palaeoclimatol. Palaeoecol.*, **560**, 110041.

Wetzel, A., **Szczygielski, A.**, **Unverricht, D.** and **Stattegger, K.** (2017) Sedimentological and ichnological implications of rapid Holocene flooding of a gently sloping mud-dominated incised valley–an example from the Red River (Gulf of Tonkin). *Sedimentology*, **64**, 1173–1202.

Wightman, D.M., **Pemberton, S.G.** and **Singh, C.** (1987) Depositional modeling of the upper Mannville (Lower Cretaceous), east-central Alberta; implications for the recognition of brackish water deposits. In: *Reservoir Sedimentology* (Eds Tillman, R.W. and Weber, J.K.), pp. 189–220. SEPM Special Publication, Tulsa, OK.

Wilson, J.G. (1990) Effects of temperature changes on infaunal circalittoral bivalves, particularly *T. tenuis* and *T. fabula*. In: *Expected Effects of Climatic Change on Marine Coastal Ecosystems*, pp. 93–97. Springer Netherlands, Dordrecht.

Yang, B.C., **Dalrymple, R.W.**, **Gingras, M.K.** and **Pemberton, S.G.** (2009) Autogenic occurrence of Glossifungites Ichnofacies: examples from wave-dominated, macrotidal flats, southwestern coast of Korea. *Mar. Geol.*, **260**, 1–5.

Yeo, R.K. and **Risk, M.J.** (1981) The sedimentology, stratigraphy, and preservation of intertidal deposits in the Minas Basin System, Bay of Fundy. *J. Sediment. Res.*, **51**, 245–260.

Zhang, L.J., **Buatois, L.A.**, **Mangano, M.G.**, **Qi, Y.A.**, **Zhang, X.**, **Sun, S.** and **Tai, C.** (2017) Early Triassic estuarine depauperate *Cruziana* Ichnofacies from the Sichuan area of South China and its implications for the biotic recovery in brackish-water settings after the end-Permian mass extinction. *Palaeogeogr. Palaeoclimatol. Palaeoecol.*, **485**, 351–360.

Zonneveld, J.-P. and **Gingras, M.K.** (2013) The ichnotaxonomy of vertically oriented, bivalve-generated equilibrichnia. *J. Paleo.*, **87**, 243–253.

Manuscript received 6 March 2024; revision accepted 9 July 2025